# 18 Optical and visual metrics

*Antonio Guirao*

## Contents

## 18.1 INTRODUCTION

The eye is a complex imaging system whose optical components determine the first step of vision. Quantifying and measuring the *ocular quality*, and how this affects the quality of the retinal images, can allow us to better understand the visual process and to improve diagnostics and correction methods. The optical quality is lowered by aberrations (consequence of the shape of the refracting surfaces), diffraction at the pupil, and scattering (due to particles and nonuniformities localized in the media). The combined effect of these three factors is that light deviates from the ideal trajectory and spreads over a deteriorated retinal image that will limit the visual performance (Artal 2014). In general, a system with less aberrations, scattering, and diffraction will produce images with higher quality. Consequently, one expects to have a better vision when images at the retina are fine. However, although the optics, the retinal image stage, and the visual perception are dependent with each other, there is not a direct or obvious relationship between these three levels. In this context, it is necessary to distinguish between optical quality, optical performance (image quality), and visual performance and to be able to define *metrics* that quantitatively measure each of these matters.

The term *performance* is used to cover all aspects of an imaging system on its ability to perform a specific task. We talk about *optical performance* to refer to the efficacy or achievement with which the optical system produces good images. The term *image quality* is used in a more restrictive sense to describe the fineness of detail that can be resolved in the image or the similarity between the image and their corresponding object. On the other hand, *visual performance* is defined by the speed and accuracy of processing visual information (CIE 2011), that is, by how well a visual task, for example, spatial vision, can be performed by a subject.

Traditional methods of assessing optical quality are defined in the *pupil plane* and account for the shape of the wave aberration (WA), for example, by means of global parameters such as the root-mean-square (RMS). On the other hand, a variety of metrics exist for specifying optical performance, based on either the *image plane* (spatial domain) or the *frequency domain*. Some of the most obvious image plane methods are intended to measure the quality of the point spread function (PSF) through scalar metrics as, for example, the Strehl ratio (SR) or the encircled energy (EE). Also, several image fidelity metrics have been developed whose goal is to measure the differences between two related images. In the Fourier or frequency domain, the modulation transfer function (MTF) represents a powerful tool for determining image quality for grating and extended objects. Meanwhile, visual performance or *subjective image quality* has been traditionally measured by means of the visual acuity and the contrast sensitivity function (CSF).

As a rule, optical quality ensures image quality and, therefore, a correct visual performance. If retinal images are good so will the vision under normal conditions (except in exceptional cases where images of extreme quality can cause visual artifacts such as aliasing). Likewise, if optics is poor, the visual perception

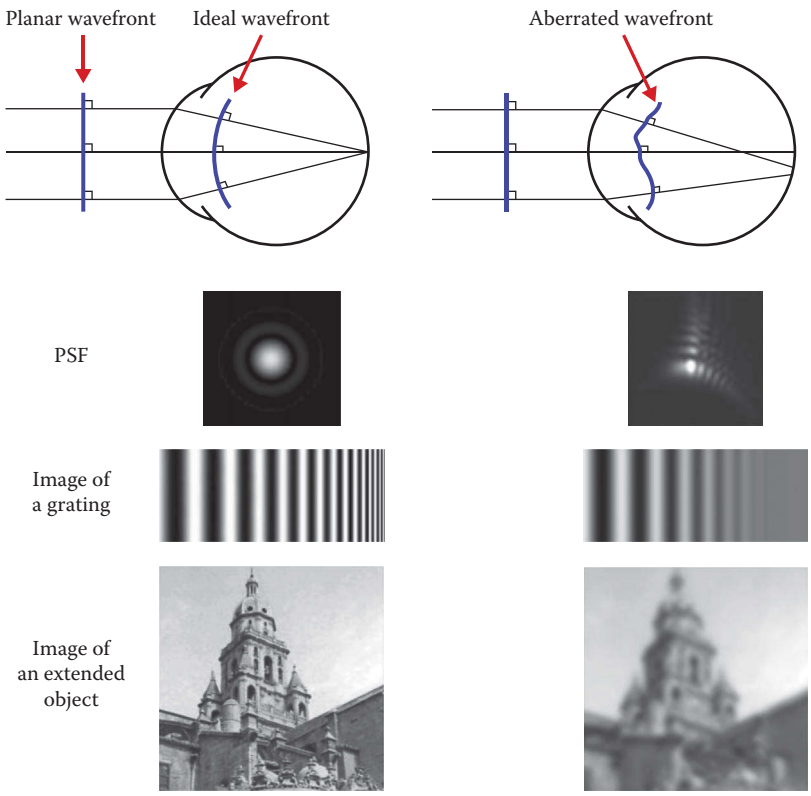


Figure 18.1 Optical wavefront, point spread function, image of a grating, and simulated image of a scene, for an ideal diffraction-limited eye and for a real aberrated eye. Different objective quality metrics may be defined based on the optical defects or based on the optical performance to form images.

will be largely limited. However, two facts should be taken into account: in some cases, a system with larger optical defects does not produce, paradoxically, worse images; and, after the optical stage of the visual processing, there are *retinal* and *neural factors* involved that explain how low-quality retinal images can still provide an acceptable visual performance. In other words, wavefront error is not always a good predictor of image quality or, for example, SR does not necessarily reflect subjective image quality. On the other hand, optical performance is relatively well matched to the capabilities of the neural network which it serves (Helmholtz 1885).

Measures of optical quality (aberrations) and optical performance (image quality, contrast transfer, etc.) are *objective methods* (Figure 18.1). While the final arbiter of image quality is the human viewer, these efforts to define objective metrics can be useful for many applications. Along with the eye, the optical performance of correcting lenses (contact, ophthalmic, and intraocular lenses), used increasingly more frequently, must be considered for understanding how the images are formed at the retina. Thus, for optical design the manufacturer needs some merit functions to achieve the quality requirements. The aberrations of the eye and their effects on retinal image quality have long been of interest. Further, the link between vision and ocular optical quality has enjoyed a renewed attention. How the complex interactions of aberrations impact visual performance is being systematically investigated by looking at correlations of objective and subjective estimates. Also, new objective metrics that incorporate some neural characteristics of the visual system have been proposed recently that correlate better with clinical measures of visual performance.

In this chapter, we present an extensive list of metrics classified into five groups (Table 18.1). Some of them are functions, such as the MTF, but most are single-value or scalar metrics such as the entropy. The first group comprises parameters of optical quality that measure the aberrations. Then, three groups of image quality metrics are described: based on the PSF, the optical performance for grating objects, and metrics that compare extended objects with their images. All metrics in these four groups are objective measures. Finally, the visual metrics in the fifth group include subjective estimates of visual performance and objective metrics based on some neural feature. One metric alone is usually not enough to describe the system appropriately. Ultimately, optical and visual performance criteria should be selected to be appropriate for the application.

## 18.2 OPTICAL QUALITY (ABERRATION-BASED) METRICS

Optical properties are typically described by an aberration or wavefront error map. See Chapter 5 of *Handbook of Visual Optics: Fundamentals and Eye Optics, Volume One* for an introduction to optical aberrations. From the WA, several pupil plane metrics can be easily computed for quantifying the optical quality both of the eye and correcting lenses.

Table 18.1 **Summarized list of metrics**

| OPTICAL QUALITY (ABERRATION BASED) | IMAGE QUALITY OF THE PSF | IMAGE QUALITY, FOURIER DOMAIN |
|---|---|---|
| WA | Strehl ratio | Contrast of grating image |
| Zernike coefficients | Intensity variance | Two-point optical resolution |
| Seidel coefficients | Peak autocorrelation | Grating optical resolution |
| RMS | Half width at half maximum | Cutoff frequency |
| Peak to valley | $1/e^2$ width | MTF |
| Pupil fractions | Width autocorrelation | Hopkins ratio |
| | Half energy diameter | Frequency for which MTF = 0.1 or 0.5 |
| | D86 diameter | Area MFT |
| | Equivalent cylinder diameter | Area Hopkins ratio |
| | Encircled energy | Pseudo Strehl ratio on MTF |
| | Second moment | Volume OTF/volume MTF |
| | Entropy | |

| VISUAL METRICS | SIMILARITY OBJECT AND IMAGE |
|---|---|
| Minimum angle of resolution | Mean square error |
| Visual acuity | Peak signal-to-noise ratio |
| Snellen fraction | Correlation coefficient |
| Maximum resolved frequency | Mutual information |
| Threshold contrast | Receiver operator characteristic |
| CSF | Structural similarity index |
| Area CSF | |
| Area MFT/NTF | |
| Subjective quality factor | |
| Area OTF/NTF | |
| Area OTF/area MTF neurally weighted | |
| Visual Strehl ratio | |
| Neural sharpness | |

### 18.2.1 POLYNOMIAL EXPANSION OF THE WAVE ABERRATION

The WA may be expressed as a polynomial expansion (Mahajan 1991), usually as a linear combination in the orthogonal variance-normalized Zernike base:

$$WA(\rho,\theta) = \sum_{n,\pm m} c_n^{\pm m} \cdot Z_n^{\pm m}(\rho,\theta) \tag{18.1}$$

where

- $\rho = r/r_o$ is the normalized radial variable (with $r_o$ the pupil radius)
- $\theta$ is the angular variable over the pupil (Malacara 1992; Wang and Silva 1980; Wyant and Creath 1992)
- $Z_n^{\pm m}(\rho,\theta)$ represent the *Zernike polynomials*
- $c_n^{\pm m}$ the *aberration coefficients*
- The subscript $n$ indicates the order of aberration (second order, third order, fourth order, etc.)
- The superscript $m$ is the angular frequency denoting the times the wavefront pattern repeats itself

Equation 18.1 can be expanded by grouping the terms according to their order:

$$WA = c_0^0 \cdot Z_0^0 + \left\{c_1^1 \cdot Z_1^1 + c_1^{-1} \cdot Z_1^{-1}\right\} + \left\{c_2^0 \cdot Z_2^0 + c_2^2 \cdot Z_2^2 + c_2^{-2} \cdot Z_2^{-2}\right\} + \left\{c_3^1 \cdot Z_3^1 + c_3^{-1} \cdot Z_3^{-1} + c_3^3 \cdot Z_3^3 + c_3^{-3} \cdot Z_3^{-3}\right\} + \left\{c_4^0 \cdot Z_4^0 + \cdots\right\} + \cdots \tag{18.2}$$

Coefficients $c_0^0$ and $c_1^{\pm 1}$, piston and tilt, are not actually true optical aberrations, as they only shift the image but do not spread light. Defocus ($c_2^0$) and astigmatism ($c_2^{\pm 2}$) are the lowest-order true optical aberrations.

During the long history of optical design, one of the most familiar approaches to merit functions has been based on *Seidel aberrations*. These are fourth-order aberrations for a system with rotational symmetry that images light coming from both on-axis and off-axis points. The WA is

$$WA_{Seidel} = A_t \rho \cos\theta_t + A_d \rho^2 + A_a \rho^2 \cos^2\theta_a + A_c \rho^3 \cos\theta_c + A_s \rho^4 \tag{18.3}$$

where the Seidel coefficients $A_t$, $A_d$, $A_a$, $A_c$, and $A_s$ represent tilt (distortion), defocus (curvature of field), astigmatism, coma, and spherical aberration, respectively. Spherical aberration affects rays from on-axis points when the optical surfaces do not have the shape needed to bring all rays to a focus. The other aberrations affect rays from points off the axis. These rays pass through a system that, from their perspective, is tilted and asymmetric; so light is not brought to a sharp focus (astigmatism and coma), images are on a curved surface instead of a flat plane (curvature of field), and, finally, images lie at a nonproportional distance from the axis (distortion).

Even for object points located on the optical axis, the WA may have the form of Equation 18.3 if the optical system has no rotational symmetry. For extension, the Seidel coefficients (some of which depend on the off-axis distance) can be related to

Zernike coefficients for on-axis aberrations. If the WA in Zernike polynomials is taken up to fourth order, the relationships between Zernike and Seidel coefficients are

$$\begin{aligned} A_t &= \sqrt{\left(2c_1^1 - 2\sqrt{8}c_3^1\right)^2 + \left(2c_1^{-1} - 2\sqrt{8}c_3^{-1}\right)^2} \\ A_d &= 2\sqrt{3}c_2^0 - 6\sqrt{5}c_4^0 - \sqrt{6}\sqrt{\left(c_2^2\right)^2 + \left(c_2^{-2}\right)^2} \\ A_a &= 2\sqrt{6}\sqrt{\left(c_2^2\right)^2 + \left(c_2^{-2}\right)^2} \\ A_c &= 3\sqrt{8}\sqrt{\left(c_3^1\right)^2 + \left(c_3^{-1}\right)^2}, \quad A_s = 6\sqrt{5}c_4^0 \end{aligned} \tag{18.4}$$

## 18.2.2 ABERRATION COEFFICIENTS AS OPTICAL QUALITY METRICS

The simplest metric for optical quality is any of the aberration coefficients, which will inform of the amplitude of a particular aberration. A single coefficient does not capture the whole optical quality because other aberrations may also be present in varying degrees. However, this way is useful in several cases, for example, when a particular aberration is dominant and responsible for the greatest loss of optical quality (e.g., in keratoconic eyes), or when we want to compare an aberration in different eyes or subjects (e.g., the degree of coma across a population), the two eyes of the same subject (e.g., the spherical aberration of both eyes), or the evolution of the aberration before and after a process (age, surgery, etc.).

The advantage of Zernike polynomials for expressing the WA is that they are linearly independent; thus, individual aberration contributions to the wavefront may be isolated and quantified separately (Figure 18.2). Further, Zernike polynomials can be identified with *balanced aberrations*, which are aberrations of a certain order mixed with other of lower order such that the variance of the net aberration is minimized. For example, the term $Z_4^0$ includes spherical aberration balanced with defocus, so the coefficient yields a WA minimal in average. In this context, examples of optical quality metrics based on single aberration coefficients can be as follows:

- The Zernike spherical aberration coefficient: $c_4^0$.
- The coma amplitude from Zernike coefficients: $\sqrt{(c_3^1)^2 + (c_3^{-1})^2}$.
- In the case of nonrotationally symmetric aberrations (e.g., coma), the orientation angle is useful besides the aberration amplitude. In general, the amplitude of a particular aberration of order $n$ and its orientation in the pupil is

$$\begin{aligned} A_n^m &= \sqrt{\left(c_n^{+m}\right)^2 + \left(c_n^{-m}\right)^2} \\ \theta_n^m &= \frac{1}{n}\arctan\left(\frac{c_n^{-m}}{c_n^{+m}}\right) \end{aligned} \tag{18.5}$$

## 18.2.3 VARIANCE AND ROOT-MEAN-SQUARE OF THE WAVE ABERRATION

The *variance*, $\sigma^2$, is a statistical parameter that measures how far a set of numbers are spread out around the mean and from each other. The variance of the WA is the mean of the squares of the WA minus the square of the mean of the WA. Mathematically,

$$\begin{aligned} \sigma_{WA}^2 &= \frac{1}{\pi}\int_0^{2\pi}\int_0^1 [WA(\rho,\theta)]^2 \rho\, d\rho d\theta - \left[\frac{1}{\pi}\int_0^{2\pi}\int_0^1 WA(\rho,\theta)\rho\, d\rho d\theta\right]^2 \\ &= \overline{WA^2} - (\overline{WA})^2 \end{aligned} \tag{18.6}$$

The square root of the variance is the *standard deviation*, $\sigma$, that measures the amount of dispersion of the WA values from the average.

One of the most practical and well-known optical quality metrics is the *root-mean-square* (RMS) of the WA. It is also a

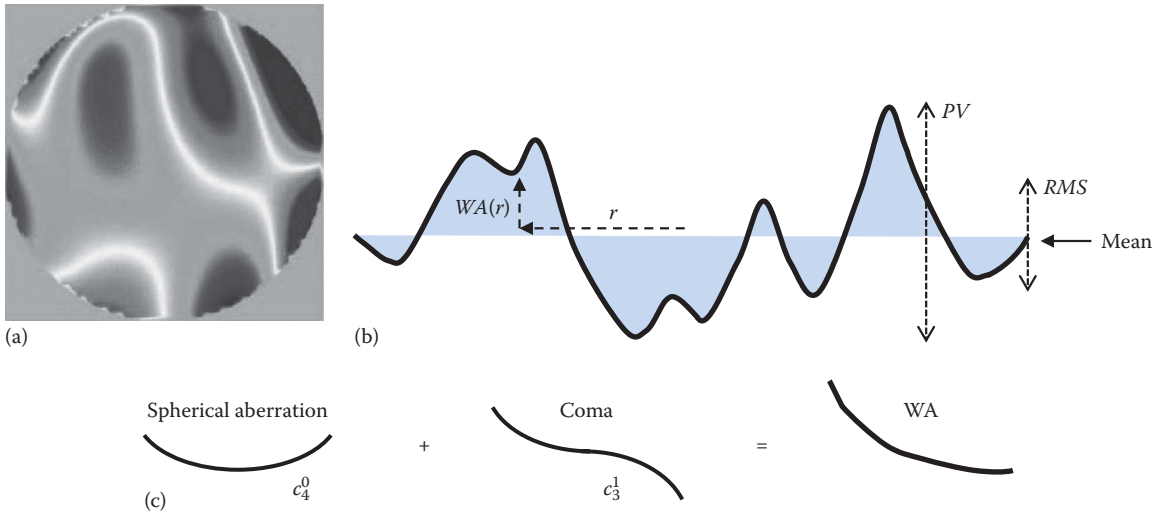


Figure 18.2 (a) Wave aberration (WA) map depicted on the pupil plane. (b) Cross section of the WA showing the deviation from the ideal aberration-free case. (c) Two different aberrations combine to give the WA. Optical quality metrics represent the magnitude of the aberrations, through polynomial expansion coefficients, variance, etc.

statistical parameter that is related to the variance and standard deviation. The name comes from its definition as the "square root of the mean of the squares" of the values. Since, in optics, the mean is always removed from the error (i.e., the WA is fixed to zero, piston term null), the variance is simply $\sigma_{WA}^2 = \overline{WA^2}$, and the RMS will equal the standard deviation:

$$RMS = \sigma_{WA} = \sqrt{\overline{WA^2}} \tag{18.7}$$

Because of the orthogonality of Zernike polynomials, the variance is given by the sum of the variance of each of the orthogonal components (Mahajan 1991). Thus, an advantage of Zernike base is that the RMS of the WA can then be obtained easily from the Zernike coefficients as

$$RMS^2 = \sum_{n,\pm m} \left(c_n^{\pm m}\right)^2 \tag{18.8}$$

In Equation 18.8, the piston term $c_0^0$ has been removed. Likewise, tilts (Zernike terms $c_1^{\pm 1}$) are removed when considering optics, since they only represent a displacement of the image, not a degradation.

The RMS metric of optical quality is based upon the principle of measuring the optical surfaces at many points and then arriving at a single number that is a statistical measure of the departure from the ideal form. This method puts into relative importance any isolated areas that may be in themselves highly deviated.

### 18.2.4 PEAK-TO-VALLEY WAVEFRONT ERROR

The *peak-to-valley* (PV) wavefront error is the maximum departure of the actual wavefront from the ideal wavefront in both positive and negative directions, that is, the distance between the maximum and the minimum values of the WA:

$$PV = \max(WA) - \min(WA) \tag{18.9}$$

This method is simple although it can be misleading because it looks at only two points and ignores the area over which the error is occurring. An optical system having a large PV error may actually perform better than other with smaller PV errors. The PV criterion became popular historically within the amateur community that used to express astronomical optics performance for mirrors, lenses, and instruments in PV terms. However, this method of rating optical quality is not representative. It is generally more meaningful to specify wavefront quality using the RMS error, as explained before.

### 18.2.5 PUPIL FRACTIONS

Some metrics of wavefront quality have been proposed based on the concept of *pupil fraction* (PF), which is defined as the fraction of the pupil area for which the optical quality is reasonably good but not necessarily diffraction limited (Thibos et al. 2004).

One of the methods for determining the area of the "good pupil" consists of taking a circular subaperture, concentric with the total pupil, within which some criterion of quality is reached (Corbin et al. 1999; Howland and Howland 1977). This subaperture is called the *critical pupil* and has a critical radius $r_c$ smaller than the pupil radius $r_o$. The PF is computed as

$$PF = \left(\frac{r_c}{r_o}\right)^2 \tag{18.10}$$

A different method is called the *tessellation method*. It consists of tessellating the entire pupil with small subapertures (e.g., about 1% of pupil diameter) and then rating each subaperture as "good" or "bad" according to some criterion. The sum of the good subapertures defines the area of the good pupil from which the PF is computed as

$$PF = \frac{\text{Area of good subapertures}}{\text{Area of the pupil}} \tag{18.11}$$

Both the critical pupil method and the tessellation method require criteria for deciding if the wavefront over a subaperture is good. The criterion for defining what is meant by good wavefront quality is somehow arbitrary and depends on the degree of optical performance expected or the specific application. For example, a criterion is that the RMS of the WA does not exceed the value of $\lambda/4$ or that a good subaperture meets $PV < \lambda/4$.

## 18.3 IMAGE QUALITY METRICS I: OPTICAL PERFORMANCE FOR POINT OBJECTS

In this section, we introduce image plane metrics that are intended to quantify the compactness, shape, and concentration of energy in the image of a point object.

### 18.3.1 THE POINT SPREAD FUNCTION

#### 18.3.1.1 Image of a point object

The *point spread function* (PSF) is the distribution of light in the image of a point object formed by an optical system for a given aberration (Mahajan 1998). The PSF is a function of two variables (coordinates at the image plane) whose values are the light intensities for each point in the image. Mathematically, the PSF is the squared modulus of the *Fourier transform* (FT) of the generalized pupil function (Goodman 1996):

$$PSF(x, y) = \left|\mathrm{FT}(P(\rho, \theta))\right|^2 \tag{18.12}$$

where $P(\rho,\theta)$ is the *generalized pupil function* defined as

$$P(\rho, \theta) = A(\rho, \theta) \cdot \exp\left[\frac{2\pi i}{\lambda} WA(\rho, \theta)\right] \tag{18.13}$$

and

$A(\rho,\theta)$ denotes a circular aperture with a unit amplitude or an optional apodization function
$WA(\rho,\theta)$ is the WA
$\lambda$ is the wavelength of the light

In general, the higher the aberrations, the more extensive the PSF and, therefore, the contrast decreases as the peak intensity drops

because light spreads over a larger area. The PSF of a diffraction-limited system is the Airy spot. Each kind of aberration produces a characteristic PSF. The eye presents a combination of all aberrations that give a PSF more or less complicated and different from one subject to another.

#### 18.3.1.2 Measuring the PSF

Today, it is relatively easy to measure the aberrations of an optical system, thanks to the aberrometry techniques, so the PSF can be calculated mathematically from the WA. Formerly, the PSF of the eye was estimated through the double-pass technique used extensively in physiological optics, which is based on recording images of a point source projected on the retina after retinal reflection and double-pass through the ocular media (Artal 2000; Iglesias et al. 1998).

For optical systems other than the eye, such as correcting lenses, the PSF can be calculated from aberration measurement or obtained directly by registration of passing light in an optical bench. However, in these cases the application of metrics based on the WA or the modulation transfer is more convenient, because when considering the effect of each element in a system as a whole, the degradation is additive in aberrations and multiplicative in contrast.

#### 18.3.1.3 Moments of the PSF: Centroid and total intensity

A *moment* is a specific quantitative measure of the shape of a function. The *n*th moment of a real-valued continuous function $f(x)$ is

$$\int x^n f(x)dx \tag{18.14}$$

If the points represent intensity values of the PSF, then the zeroth moment is the total energy, the first moment divided by the total energy is the center of mass, and the second moment is the inertia.

The *centroid*, or center of mass, of the PSF is the point where the light of the image could be concentrated. The coordinates $(\bar{x}, \bar{y})$ of the centroid are computed as the arithmetic mean position of all the points in the PSF shape:

$$\bar{x} = \frac{\iint_{image} x\, PSF(x,y)dxdy}{Vol(PSF)}, \quad \bar{y} = \frac{\iint_{image} y\, PSF(x,y)dxdy}{Vol(PSF)} \tag{18.15}$$

where $Vol(PSF) = \iint_{image} PSF(x,y)dxdy$ is the volume or total intensity energy in the image. In aberrated systems, the centroid of the PSF may not coincide with the coordinate origin.

The *normalized point spread function*, $PSF_N$, is defined with total intensity equal to 1:

$$PSF_N = \frac{PSF}{Vol(PSF)} \tag{18.16}$$

The normalized PSF may be seen as a probability density function. Then, the zeroth moment of $PSF_N$ is the total probability (i.e., 1), the first moment is the mean, the second moment is the *variance*, and the third moment is the *skewness*.

#### 18.3.1.4 The Airy disk of diffraction: Diffraction-limited PSF

The *Airy pattern* is the best focused spot of light that a perfect system with a circular pupil can make, limited by the diffraction of light, that is, the PSF for an unaberrated system. The *Airy disk* is the central core of the Airy pattern. It contains a maximum of 84% of the light entering the optical system. The angular radius of the Airy disk is

$$\theta_{Airy} = 1.22\frac{\lambda}{D} \tag{18.17}$$

where

$\lambda$ is the wavelength of the light
$D$ is the diameter of the pupil

### 18.3.2 STREHL RATIO AND INTENSITY SHARPNESS METRICS

#### 18.3.2.1 Strehl ratio

The *Strehl ratio* (SR) is defined as the ratio of the intensity value at the center of the image with and without aberrations for the same pupil size:

$$SR = \frac{PSF(0,0)}{PSF_{d-l}(0,0)} \tag{18.18}$$

where $PSF_{d-l}$ is the aberration-free diffraction-limited PSF. Strehl performance is usually expressed as a range of numbers from 1 to 0. A perfect system is 1, a completely imperfect system is 0, and acceptable standards occur somewhere in between.

The SR has been in regular use for many years and describes one of the most common and significant measures of optical performance. Although the mathematics involved in the calculation of the SR may be complex, they can be rather easily explained in concept. Once the PSF is available, the SR is really quite easy to relate to and is simple to understand. However, characterizing image quality by this single number will be meaningful only if the PSF is little distorted, which is true for a well-corrected system that operates close to the diffraction limit. For small aberrations, the SR and the RMS of the WA correlate well with each other. Several equations have been derived for expressing this relationship for low aberrations (SR down to values of about 0.5); one of the best known is (Mahajan 1982)

$$SR \approx e^{-\left(\frac{2\pi}{\lambda}RMS\right)^2} \approx 1-\left(\frac{2\pi}{\lambda}RMS\right)^2 \tag{18.19}$$

where $\lambda$ is the wavelength. However, only for large SR values the intensity is maximum at the point associated with minimum aberration variance. For large aberrations, there is no simple relationship between the SR and the aberrations.

An alternate definition of SR is often given in terms of the peak intensity ($SR_{peaks}$), so this metric is defined as the ratio of the maximum value of the PSF in the presence and absence of aberrations:

$$SR_{peaks} = \frac{\max(PSF)}{\max(PSF_{d-l})} \tag{18.20}$$

The peak of the *PSF* does not necessarily occur at the coordinate origin, specially for large and nonsymmetrical aberrations. Consequently, the $SR_{peaks}$ is not equivalent in general to the actual SR.

#### 18.3.2.2 Other intensity sharpness metrics

The SR refers to a single value of the PSF, its maximum value. It may happen that the PSF has a high peak value but the light is widely distributed (i.e., a bad image). Other metrics attempt to measure the sharpness of the PSF considering all the intensity values over the entire image (Figure 18.3). These metrics are, indirectly, an estimate of the spatial resolution since a sharper PSF will blur the image less. In particular, we will introduce here: intensity variance and autocorrelation. Other sharpness metrics can be found in the literature (Fienup and Miller 2003).

The *intensity variance of the PSF* summarizes in one number the histogram of intensity values of the PSF. Variance measures how far the values are spread out from the average. A variance of zero indicates that all the values are identical (i.e., a flat completely blurred PSF); on the contrary, a sharp image has a high variance. The intensity variance of the PSF is calculated as the average value of the squared PSF minus the average PSF squared:

$$\sigma_{PSF}^2 = \overline{PSF^2} - \overline{PSF}^2 \qquad (18.21)$$

The *standard deviation of the PSF*, $\sigma_{PSF}$, is the square root of the variance.

*Peak of the autocorrelation of the PSF*: The autocorrelation is the cross-correlation of the PSF with itself:

$$C(x,y) = PSF \otimes PSF = \iint_{image} PSF(s,t)PSF(s-x,t-y)\,ds\,dt \qquad (18.22)$$

A high spatial autocorrelation indicates that there are small differences between the values of the PSF in nearby points and large differences between distant points, that is, a smooth sharp PSF will have a narrow autocorrelation function. In this context, a metric for sharpness is the peak of the autocorrelation function.

### 18.3.3 METRICS FOR SPATIAL COMPACTNESS OF THE PSF

Some scalar metrics are designed to capture the attributes of spatial compactness of the PSF such that small values of the metric indicate a compact PSF of good quality. The most used are defined in the following (Figure 18.3).

#### 18.3.3.1 Width metrics, referred to peak value and sharpness

The *full width at half maximum* (FWHM) is an expression of the extent of the PSF given by the distance between points on the curve at which the intensity reaches half its maximum value. *Half width at half maximum* (HWHM) is half of the FWHM (Charman and Jennings 1976; Westheimer and

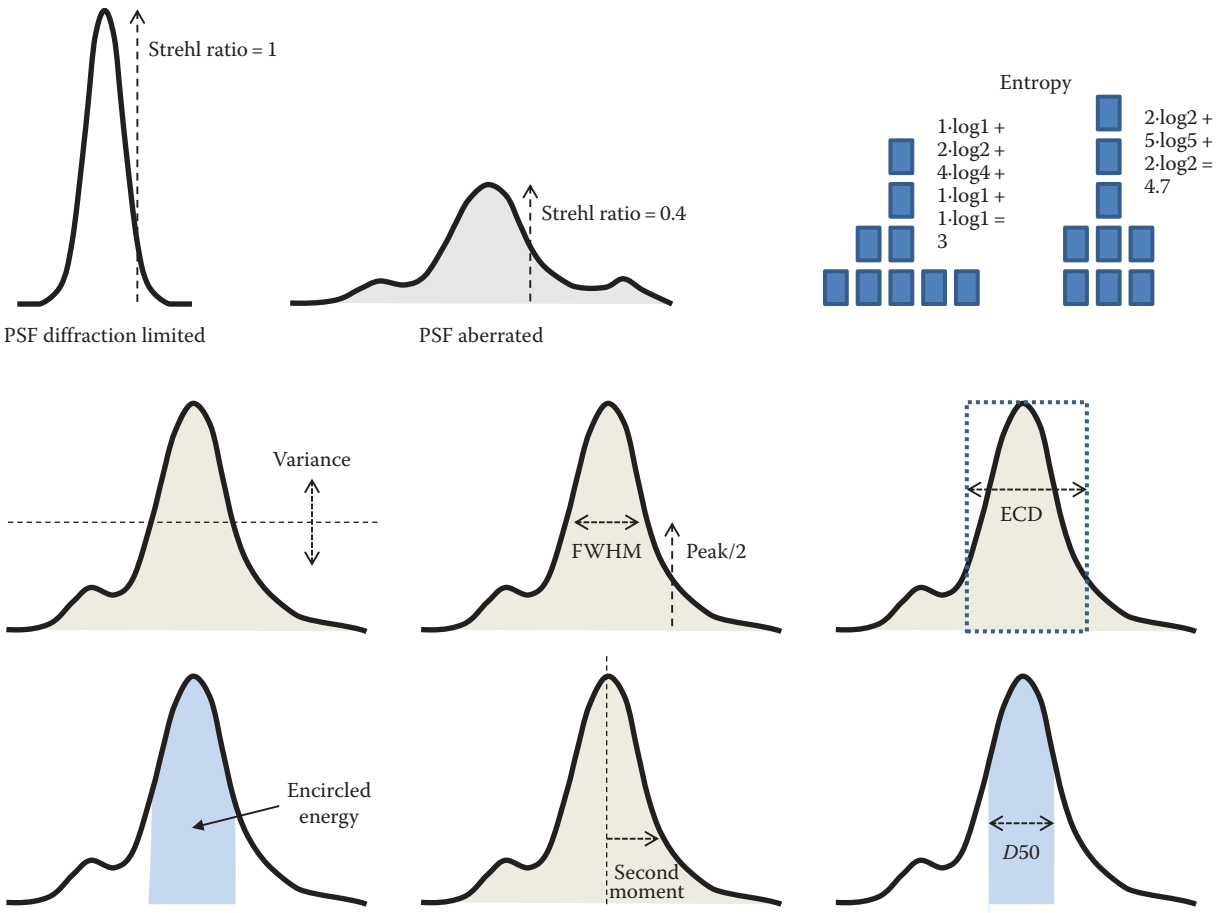


Figure 18.3 Cross sections of the point spread function (PSF) showing the idea behind different image quality metrics that account for the compactness, shape, and energy concentration of the PSF.

Campbell 1962). If the PSF is expressed in polar coordinates, the HWHM is computed as the average width of every cross section of the PSF:

$$HWHM = \sqrt{\frac{1}{\pi}\int_0^{2\pi}\int_0^{\infty}\Pi(r,\varphi)r\,dr\,d\varphi} \qquad (18.23)$$

where $\Pi(r, \varphi) = 1$ if $PSF(r, \varphi) > \max(PSF)/2$, otherwise $\Pi(r, \varphi) = 0$.

Similarly, the *1/e² width* is equal to the distance between the two points on the PSF distribution that are $1/e^2 = 0.135$ times the maximum value.

*Width of the PSF autocorrelation*: This metric is the HWHH of the autocorrelation $C(x,y)$ of the PSF. A similar metric is the *width of the correlation of the PSF with the diffraction-limited PSF* that is used as reference.

#### 18.3.3.2 Diameter metrics, referred to encompassed energy

The *half energy diameter* ($D50$) is the diameter of a circular area centered on the PSF peak that captures 50% of the light energy. This diameter is computed from the implicit radius $r = D50$ that is the limit of the definite integral

$$\int_0^{D50}\int_0^{2\pi} PSF_N(r,\varphi)r\,dr\,d\varphi = 0.5 \qquad (18.24)$$

where $PSF_N$ is the normalized PSF with intensity = 1 and peak value located at $r = 0$.

The *D86 diameter* is defined as the diameter of the circle that is centered at the centroid of the PSF profile and contains 86% of the total energy. In this case, we must do first a translation of the PSF so it is centered at the centroid. The D86 width is often used in applications that are concerned with knowing exactly how much power is in a given area, for example, applications of laser beams (Siegman 1998). The percentage of 86 is chosen because a circular Gaussian beam profile integrated down to $1/e^2$ of its peak value contains 86% of its total power.

*The equivalent diameter* (ECD) is the diameter of the circular base of that cylinder that has the same volume as the PSF and the same height. If the normalized PSF is taken, the value of ECD is given by

$$ECD = \sqrt{\frac{4}{\pi\max(PSF_N)}} \qquad (18.25)$$

#### 18.3.3.3 Asymmetry of the PSF: Skewness

*Skewness* is a measure of the degree of asymmetry of the distribution of light in the PSF. If the left tail is longer than the right tail (the light of the distribution is concentrated on the right), the function has negative skewness and is said to be left-skewed or left-tailed. If the reverse is true, it has positive skewness (the right tail is longer; the light is concentrated on the left) and the distribution is said to be right-skewed or right-tailed.

The skewness is the third moment of the PSF. It can be calculated as the average of every cross section of the PSF centered at $r = 0$:

$$\text{Skewness} = \frac{1}{\pi}\int_0^{\pi}\left[\int_{-\infty}^{\infty} r^3\,PSF(r,\varphi)dr\right]d\varphi \qquad (18.26)$$

### 18.3.4 CONCENTRATION OF LIGHT

#### 18.3.4.1 Encircled energy

The optics term *encircled energy* (EE) measures the fraction of the total energy in the PSF that lies within a circle of specified radius (Shannon 1997; Srisailam et al. 2011). It is calculated by first determining the total energy of the PSF over the full image plane and the centroid. Circles of increasing radius are then created at the centroid and the energy within each circle is calculated and divided by the total energy. As the circle increases in radius, more of the PSF energy is enclosed. The EE curve thus ranges from zero to one. The EE in a circle of radius $R$ is

$$EE(R) = \int_0^{R}\int_0^{2\pi} PSF_N(r,\varphi)r\,dr\,d\varphi \qquad (18.27)$$

A typical criterion for EE is the radius of the PSF at which either 50% or 80% of the energy is encircled. Also, it is often considered the EE that falls within the core corresponding to the Airy disk; in this case the EE is called *light-in-the-bucket* (Thibos et al. 2004).

#### 18.3.4.2 Second moment of intensity distribution

The *second moment of the PSF* ($M2$), also known as moment of inertia, measures the concentration of light in the near vicinity of the center (Bareket 1979). It represents the spatial variance of the PSF. If the normalized PSF is taken, the moment of inertia is

$$M2 = \int_0^{\infty}\int_0^{2\pi} r^2 PSF_N(r,\varphi)r\,dr\,d\varphi \qquad (18.28)$$

#### 18.3.4.3 Entropy of the PSF

This metric is inspired by an information theory approach to optics (Barakat 1998; Bove 1993; Guirao and Williams 2003). The *entropy* ($H$) is mathematically calculated as follows (Shannon entropy):

$$H = -\sum_{x,y} PSF_N(x,y)\cdot\log PSF_N(x,y) \qquad (18.29)$$

where log is the decimal logarithm.

The entropy is a measure of the spatial variance of the PSF, that is, a measure of how the energy is distributed in the image. The aberration-free PSF shows the minimum entropy with the maximum concentration of light in the center. Aberrations increase the entropy because light tends to spread throughout the image. An image with an intensity constant level has the maximum entropy. Both the second moment and the entropy are metrics sensitive to the shape of the PSF tails (Figure 18.3).

## 18.4 IMAGE QUALITY METRICS II: OPTICAL PERFORMANCE FOR GRATING OBJECTS, METRICS BASED ON THE FOURIER DOMAIN

In the previous section, we have introduced image quality metrics based on the degraded image of point objects. However, in the real world, except when, for example, we look at stars, it is common to find extended objects with complicated light distributions. A method for studying the optical performance is based on the reduction of contrast that the optical system produces on the image of objects having a particular pattern detail. For that purpose, the Fourier analysis is a useful and powerful tool (Goodman 1996; Mahajan 1998; Williams 1998; Williams and Becklund 2002). By means of the so-called Fourier transform, complicated signals may be written as the sum of simple waves mathematically represented by sines and cosines. Significant simplification is often achieved by transforming spatial functions, such as intensity distributions, to the frequency domain of the Fourier space, which manifests the periodic information contained in the signal.

### 18.4.1 PERIODIC PATTERNS: CONTRAST AND OPTICAL RESOLUTION

#### 18.4.1.1 Basics of gratings

In the study of visual perception, periodic patterns (sine and square-wave gratings) are frequently used to probe the capabilities of the visual system. A *grating* is a repeating sequence of light and dark. One adjacent pair of a light and a dark strip makes up one cycle. These cycles repeat over and over in a grating. A *sine-wave*, or sinusoidal, grating shows a smooth repetitive sine-shaped oscillation. A *square-wave* grating is a nonsinusoidal periodic waveform in which the amplitude alternates at a steady frequency between fixed minimum and maximum values, that is, it is composed of black and white bars.

Three parameters define periodic patterns (in our case, objects with periodic distributions of light and their images): spatial frequency, contrast, and phase.

The *spatial frequency* ($f$) is a measure of how often periodic components of the pattern repeat per unit of distance or angle. Spatial frequency is often expressed in units of cycles per millimeter, or cycles per degree of visual angle.

The *contrast* ($C$), or modulation, is a measure of the difference between the extreme intensity values and the average intensity. *Michelson contrast* is defined as

$$C = \frac{I_{max} - I_{min}}{I_{max} + I_{min}} \tag{18.30}$$

where $I_{max}$ and $I_{min}$ are the maximum and minimum values of intensity in the pattern (object or image). A pattern with a flat or uniform intensity profile has contrast null. Conversely, a pattern with contrast unity presents minimum intensity values equal to zero.

The *phase* of the object, or image, is the shift (expressed in radians or degrees) of the location of the peak of the signal from the origin.

In general, extended objects are not as simple as a grid, but contain many spatial frequencies. In that case, the light distribution is decomposed by Fourier analysis as a combination of multiple gratings.

#### 18.4.1.2 Contrast as a metric

If, in particular, one is considering the response of the optical system to a grating object of known contrast, a single-value metric is simply the Michelson contrast in the grating image as defined earlier, or the relative contrast between object and image (Figure 18.4). The generalization of this metric for grating objects with any spatial frequency will lead in the next section to introduce the MTF.

#### 18.4.1.3 Two-point optical resolution

Often the quality of an imaging system is expressed in terms of *optical resolution*, which describes the ability of the system to resolve small details in the object that is being imaged (Born and Wolf 1999). The spatial, or angular, resolution is based on the minimum separation, or angle, at which two details (points, lines, stars, etc.) can be distinguished as individuals.

One requires empirical criteria to quantitatively calculate optical resolution. Several objective criteria have been used in classical optics, most taken from astronomy where they had a very practical significance. One of the standards is based on the *Rayleigh criterion of resolution* and states that two points are considered to be just resolved when the distance between them is such that, on the midpoint between the image of one point and

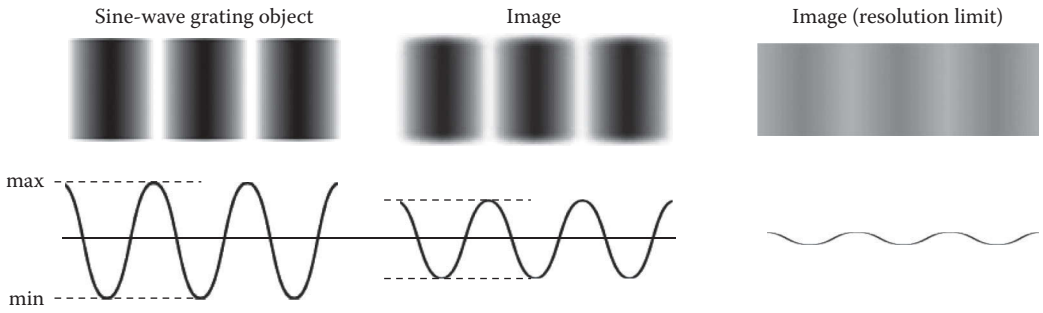


Figure 18.4 Contrast of gratings. The contrast measures the difference between the extreme intensity values and the average intensity in an image. When the degradation is large, the contrast tends to zero until finally the stripes in the grating image become indistinguishable (concept of grating optical resolution).

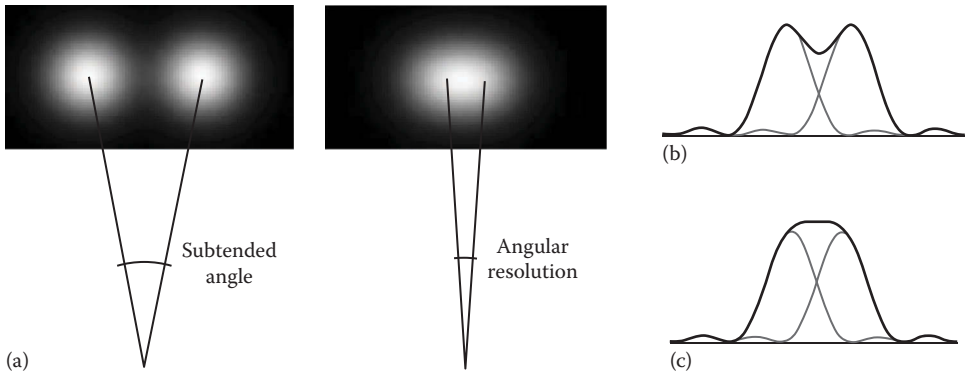


Figure 18.5 (a) Two-point optical resolution. (b) Rayleigh's resolution criterion. (c) Sparrow's resolution criterion.

the next, the intensity be 0.74% of the peak, that is, the contrast be 15% lower than the maximum.

The *Sparrow's resolution criterion* improves on this by saying that resolution is reached when the combined image of the two points no longer has a dip in brightness between them but instead has a roughly constant brightness from the peak of one image to the other (Figure 18.5). The Rayleigh criterion is more strict, while the alternate Sparrow criterion corresponds better with what the human eye can resolve.

The upper limit for two-point optical resolution is achieved for aberration-free optical systems. In this ideal case, the image of a point object is the diffraction Airy PSF and the angular resolution for the Rayleigh and the Sparrow criteria are given, respectively, by

$$\theta_{\substack{Rayleigh \\ d-l}} = 1.22\frac{\lambda}{D}, \quad \theta_{\substack{Sparrow \\ d-l}} = 0.95\frac{\lambda}{D} \tag{18.31}$$

where

λ is the wavelength of the light
$D$ is the diameter of the lens's aperture
The angle is expressed in radians
The subscript $d-l$ means the diffraction-limited ideal case

#### 18.4.1.4 Grating optical resolution and cutoff frequency

When considering gratings, resolution aims to the minimum spatial frequency in the grating object that can be resolved in its image. In this case, one often speaks of *grating optical resolution*. Thus, resolution is usually expressed in terms of lines per millimeter or cycles per degree, where a "line" or cycle is a sequence of one black strip and one white strip. The inverse of the frequency yields the spacing between two resolved details (two black or two white stripes). One can say, for example, that an optical system resolves 30 cycles per degree; the meaning of this is that two successive light stripes (or two successive dark stripes) separated by 1/30 degrees (= 2 minutes of arc) may be distinguished in the image, based on some objective criterion such as the Rayleigh or the Sparrow.

An upper limit to the objective estimate of grating optical resolution is given by the so-called cutoff frequency ($f_{cutoff}$), that is, the spatial frequency of a grating at which contrast in the image reaches zero and the details have disappeared completely. The maximum value for the cutoff frequency that can be achieved corresponds to a perfectly corrected (diffraction-limited) optical system and is given by

$$f_{\substack{cutoff \\ d-l}} = \frac{D}{\lambda} \text{ cycles/rad}, \quad \text{or} \quad f_{\substack{cutoff \\ d-l}} = \frac{\pi}{180}\frac{D}{\lambda} \text{ cycles/degree} \tag{18.32}$$

One can see that the inverse of $f_{\substack{cutoff \\ d-l}}$ is very close to the angular resolution $\theta_{\substack{Sparrow \\ d-l}}$.

#### 18.4.1.5 Drawbacks of the optical resolution methods

Resolution is a metric for measuring directly, by means of a single value, the performance of optical systems such as contact, intraocular, and ophthalmic lenses. In the case of the eye, the retinal image is not accessible and, then, resolution can only be estimated from the MTF measured indirectly or calculated from the ocular aberrations.

A weakness of the optical methods is that resolution is a threshold detection process. The criteria mentioned earlier are somehow arbitrary when applied to the human visual system. Ultimately, it is necessary to consider retinal and neural factors for knowing whether or not two objects may be resolved depending on their separation and contrast. This leads us to later define the visual resolution.

Another drawback is that objects in the real world are in general of relatively low contrast, so that the resolution limit obtained using high-contrast test patterns can be meaningless. The MTF and its psychophysical counterpart, the CSF, have a much complete information of the size of detail one might expect the eye to resolve in normal use.

### 18.4.2 OPTICAL TRANSFER FUNCTION AND MODULATION TRANSFER FUNCTION

#### 18.4.2.1 Optical transfer function

The *optical transfer function* (OTF) specifies the translation and contrast reduction of a periodic sine pattern after passing through the optical system, as a function of its periodicity and orientation. Formally, the OTF is defined as the FT of the PSF (Goodman 1996; Mahajan 1998):

$$OTF(u,v) = FT(PSF(x,y)) \tag{18.33}$$

where $(u, v)$ are the spatial frequencies of the pattern along two perpendicular directions.

Because of the relationship of Equation 18.12 between the PSF and the pupil function of the system, the OTF is also given by the autocorrelation of the pupil function:

$$OTF(u,v) = P \otimes P = \iint_{pupil} P(s,t)P^*(s-u,t-v)ds\,dt \quad (18.34)$$

where the asterisk indicates a complex conjugate. Thus, the OTF of a system can be obtained from its WA without having to calculate the PSF.

The OTF is a complex valued function. The absolute value is commonly referred to as the *modulation transfer function* (MTF), which gives the relative contrast between the image and the object. On the other hand, when also the pattern translation is important, the complex argument of the OTF can be depicted as a second real-valued function, commonly referred to as the *phase transfer function* (PTF), that indicates a change in the location of the peak of the pattern. The OTF in terms of the MTF and PTF is

$$OTF(u,v) = MTF(u,v)\cdot e^{i\,PTF(u,v)} \quad (18.35)$$

A high-quality OTF is indicated by high MTF values and low PTF values.

The OTF provides a comprehensive and well-defined characterization of optical systems (Williams 1998). Any object can be conceived as the sum of gratings of various spatial frequencies, contrasts, phases, and orientations. The optical system of the eye is a filter that reduces the contrast and changes the relative position of each grating in the object spectrum.

#### 18.4.2.2 Modulation transfer function

This function is a measurement of the ability of an optical system to transfer modulation or contrast at a particular spatial frequency from the object to the image (Figure 18.6). Mathematically, it is the modulus of the FT of the PSF:

$$MTF = |FT(PSF)| \quad (18.36)$$

The MTF is a function of a two-dimensional spatial frequency coordinate, $(u,v)$. A one-dimensional MTF may be computed radially averaging the values across all angles:

$$MTF(f) = \frac{1}{2\pi}\int_0^{2\pi} MTF(f,\varphi)d\varphi \quad (18.37)$$

where the radial spatial frequency is $f = \sqrt{u^2+v^2}$. In this one-dimensional MTF, the *Y*-axis is the contrast transferred by the eye's optics, and the *X*-axis represents sine waves with spatial frequency ($f$) varying from low (large spacing between adjacent white stripes) to high (fine gratings):

$$MTF(f) = \frac{C_{image}(f)}{C_{object}(f)} \quad (18.38)$$

The MTF accounts for optical performance in terms of contrast. High contrasts at low spatial frequencies reproduce perfectly large image details, while high contrasts at high frequencies drive how well smaller details are seen. For the human eye, the contrast of the image decreases as the spatial frequency increases.

The MTF is an important tool for the objective assessment of the image-forming capability of optical systems. Resolution metrics represent the limit of the eye to resolve details, given that the image is shown with 100% contrast. However, the MTF accounts for the contrast over the full range of spatial frequencies.

### 18.4.3 METRICS BASED ON THE MTF

#### 18.4.3.1 Diffraction-limited MTF and Hopkins contrast ratio

The *diffraction-limited MTF* ($MTF_{d-l}$) is the MTF for a system in which the effects of optical aberrations are assumed to be negligible. An optical system cannot perform better than its $MTF_{d-l}$ because any aberrations will pull the MTF curve down. The $MTF_{d-l}$ represents the upper limit to the eye's performance, and it is based on the overall limiting pupil aperture and the wavelength of the light. The *cutoff frequency* for the $MTF_{d-l}$ was defined before (Equation 18.32) as the spatial frequency for which

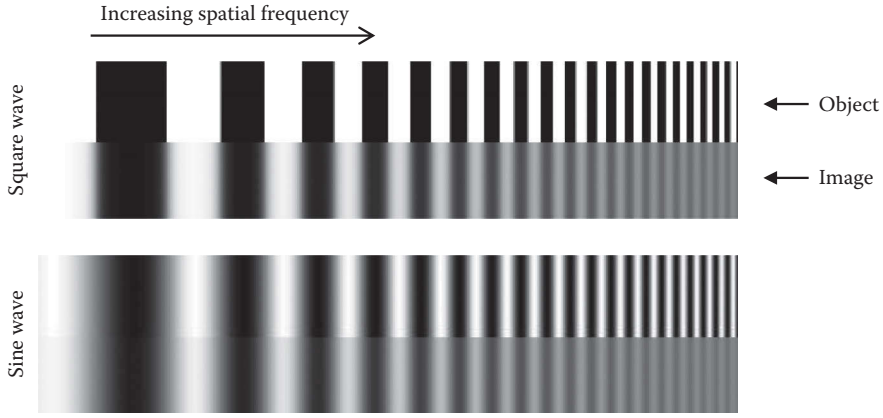


Figure 18.6 The modulation transfer function indicates the reduction of contrast from the object to the image for each spatial frequency. This reduction is shown in the figure for a square-wave grating and for a sine-wave grating.

the contrast becomes zero in the ideal case of an unaberrated system ($f_{cutoff\,MTFd-l} = D/\lambda$ cycles/rad).

The *Hopkins ratio* (HR), or Hopkins contrast ratio, is often used to characterize the image quality of an optical system. It is defined as the actual aberrated MTF divided by the diffraction-limited MTF as a function of spatial frequency (Hopkins 1966; Mahajan 1991):

$$HR(f) = \frac{MTF(f)}{MTF_{d-l}(f)} \tag{18.39}$$

Some authors use the term *optical quality factor* instead of HR when referring to this metric (Lisson and Mounts 1992).

### 18.4.3.2 Single values from the MTF

Instead of a complete curve MTF from zero to the cutoff frequency ($f_{cutoff\ MTF}$), in many cases, it is enough considering a limited range of spatial frequencies or, in some instances, picking out single MTF values at a few important frequencies.

A hint is to discard the MTF at low spatial frequencies because differentiation between high-performance and low-performance systems is difficult in this region. The high frequencies just under cutoff could be also avoided because even for well-corrected eyes the contrast is so small that erratic behavior in this region is usually of little consequence. Since the eye is relatively insensitive to detail at high spatial frequencies, a criterion consists of taking as an image quality metric the *spatial frequency at which MTF decreases to 10% level*. Experience has shown that the best indicators of image sharpness are the spatial frequencies at which the contrast attenuates by 50%, so an alternate metric is the *spatial frequency corresponding to the MTF equal to 0.5* (MTF50). Some works have considered the MTF value at the intermediate frequencies of 16 and 32 cycles/degree.

### 18.4.3.3 Area under the MFT or under the Hopkins ratio

While the MTF captures a lot of information about an imaging system, it is desirable to describe performance with a single figure of merit or scalar metric instead of a function. The area under the MTF has been one of the heavily researched metrics of image quality for the human eye. The image quality is directly linked to the integrated MTF curve between zero and the absolute limiting frequency, $f_{cutoff\ MTF}$, which means the richness of the information contained in the image is a function of the area below the MTF curve. An alternative is to use the area of the HR curve.

Other approaches have been used. One is considering the area between spatial frequencies of 0 and 60 cycles/degree, or between 5 and 30 cycles/degree (Figure 18.7).

### 18.4.3.4 Strehl ratio from the Fourier domain

The SR defined in Equation 18.18 can be also calculated in the Fourier or frequency domain as the normalized volume under the OTF of the aberrated system:

$$SR = \frac{PSF(0,0)}{PSF_{d-l}(0,0)} = \frac{\int_{-\infty}^{\infty}\int_{-\infty}^{\infty} OTF(u,v)\,du\,dv}{\int_{-\infty}^{\infty}\int_{-\infty}^{\infty} OTF_{d-l}(u,v)\,du\,dv} \tag{18.40}$$

where $OTF_{d-l}$ is the diffraction-limited OTF.

In many cases the PTF is unknown, which has led to the substitution of the MTF for the OTF in the previous calculation. Although this lacks rigorous justification, it is a popular method for defining a scalar metric ($SR_{MTF}$) once one knows the MTF. In particular, from the radially averaged MTF we can define (Driggers 2003)

$$SR_{MTF} = \frac{\int_{0}^{\infty} MTF(f)df}{\int_{0}^{\infty} MTF_{d-l}(f)df} \tag{18.41}$$

This metric is similar to the true SR but it is not the same, and it is also different to the $SR_{peaks}$ defined in Equation 18.20.

### 18.4.3.5 Phase shifts and PTF

Most image quality metrics do not use phase in their calculation. The PTF tells how much the detail at each spatial frequency is shifted on the image relative to that detail on the object plane. In a nonsinusoidal extended object, the distribution of light can be broken down into sinusoidal components by Fourier methods. To preserve the exact appearance of the pattern, the sinusoidal

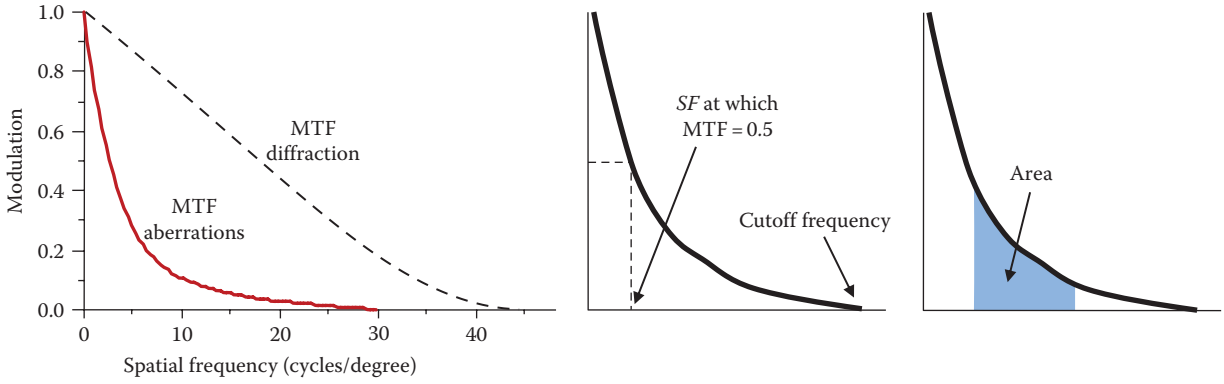


Figure 18.7 Modulation transfer function (MTF) for a real eye in comparison with the diffraction-limited MTF. Some examples of metrics based on the modulation transfer are spatial frequency at which the MTF decreases to 50%, cutoff frequency (*MTF* = 0), area under the MTF, and Hopkins ratio = quotient between MTF and diffraction MTF.

components must be kept in their original positions, which requires a linear PTF curve. Nonlinearities in the PTF, also called phase distortion, cause different spatial frequencies in the image to recombine with different relative phases.

No general statement can be made concerning the degradation of image quality caused the PTF. For certain cases, the PTF may supplement the information given by the MTF, but the PTF alone usually conveys little information. A metric that is intended to quantify phase shifts in the image is defined as the volume under the OTF normalized by the volume under the MTF (Thibos et al. 2004):

$$\frac{Vol(OTF)}{Vol(MTF)} = \frac{\int_{-\infty}^{\infty}\int_{-\infty}^{\infty} OTF(u,v)\,dudv}{\int_{-\infty}^{\infty}\int_{-\infty}^{\infty} MTF(u,v)\,dudv} \tag{18.42}$$

### 18.4.4 MEASURING RESOLUTION AND MTF

A variety of test targets are available for measuring resolution (Smith 2000). These targets consist of equally spaced white and black bars. The widest bar the imager cannot discern, according to some resolution criteria, is the limitation of its resolving power. For example, the *Ronchi ruling*, or Ronchi grating, is a constant-interval alternating bar and space square-wave target that has a high edge definition and contrast ratio. Another of the existing test used for optical testing purposes is the *USAF 1951 resolution test target*. The pattern consists of groups of three bars with dimensions from big to small (covering a range of 0.25–228 cycles/mm) at different orientations.

The MTF for the eye can be obtained theoretically from WA measurements or double-pass PSF registration. In the case of correcting lenses, the MTF can be also measured directly by means of interferometry or by using sinusoidal grating objects.

As noted several times, one drawback of objective methods for assessing the visual performance is that they neglect the retinal and neural factors of the human visual system. However, a characteristic of the MTF is that it illustrates how well the eye could reproduce the contrast of the observed scene after the major limit imposed by the optical factors. In this sense, the MTF is objective and universal. Moreover, the MTF can be calculated from ocular aberration data giving scientists the ability to study the diffraction–aberration effects for different spatial frequencies and to design correcting lenses or surgery techniques for improving the optical quality. Another benefit is that the resulting MTF of a compound optical system is the product of all the MTF of its individual components, allowing researchers and manufacturers the comparison of the image quality with the expectations from the design stage and the prediction of system performance reliably.

## 18.5 IMAGE QUALITY METRICS III: SIMILARITY BETWEEN OBJECT AND IMAGE

As the ocular system forms a deteriorated image in the retina, the original object and its retinal image can be compared. The more similar these two images are, the better the optical performance.

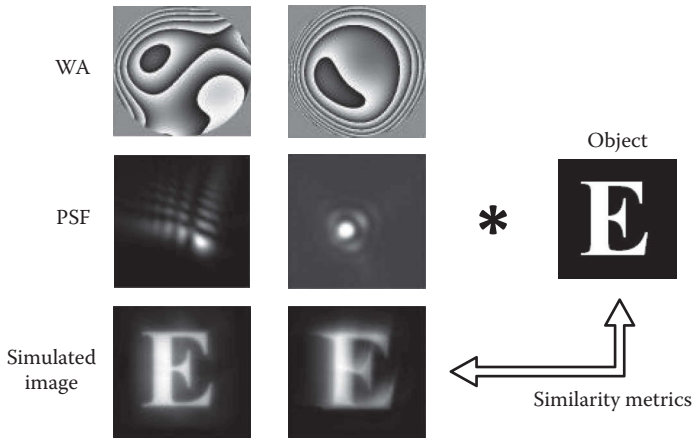


**Figure 18.8** Convolution of a letter E with the point spread function calculated from the wave aberration data of two subjects. The simulated image and the reference image may be compared through several fidelity parameters such as the mean square error and the correlation coefficient.

The object can be a generated digital image of a real scene ($O$). Then, the corresponding retinal image ($I$) can be estimated computationally by convolving the eye's PSF with the object using the standard Fourier calculus. When the two images are available, the original and degraded, the following metrics may be used for measuring similarity and, therefore, estimating image quality (Figure 18.8).

### 18.5.1 SIMULATED IMAGES OF EXTENDED OBJECTS: CONVOLUTION

Mathematically, we may represent a complex or extended object as a sum over weighted impulse functions. The PSF may be independent of position in the object plane, in which case it is called shift invariant (Wandell 1995). In addition, if there is no distortion in the system, the image plane coordinates are linearly related to the object plane coordinates via the magnification $M$. Thus, the image of an extended object can be calculated as a superposition of weighted PSFs through a straightforward operation:

$$I(x,y) = \iint O(u,v)\cdot PSF(u-x/M, v-y/M)\,dudv \tag{18.43}$$

where $O(u,v)$ and $I(x,y)$ represent the object and image, respectively. This integral is called *convolution*. So, the image of a complex object can be seen as a convolution of the true object and the PSF:

$$I = O * PSF \tag{18.44}$$

### 18.5.2 FULL-REFERENCE METRICS

*Full-reference* metrics compute the quality difference by comparing every pixel of the distorted image to its corresponding pixel in the original object (Zhang et al. 2012).

#### 18.5.2.1 Mean square error between object and image

The simplest and most widely used full-reference quality metric is the *mean squared error* (MSE), computed by averaging the squared intensity differences of distorted and reference image pixels (Gonzalez 2008):

$$MSE = \frac{1}{n}\sum_{i=1}^{N}(O_i - I_i)^2 \tag{18.45}$$

where

$N$ is the number of pixels

$O_i$ and $I_i$ are the intensity values in the pixel $i$

#### 18.5.2.2 Peak signal-to-noise ratio

The related quantity of *peak signal-to-noise ratio* (PSNR) is an engineering term for the ratio between the maximum possible power of a signal and the power of corrupting noise that affects the fidelity of its representation. From the MSE, the PSNR is defined as

$$PSNR = 10 \cdot \log \frac{(MAX_O)^2}{MSE} \tag{18.46}$$

with $MAX_O$ being the maximum possible pixel value of the reference object $O$ (e.g., when the pixels are represented using 8 bits per sample, this is 255).

Both MSE and PSNR can fail if the data diverge too much from the ideal case. It is well established that, in general, these simple approaches do not provide meaningful measures of image fidelity, and more sophisticated techniques are necessary.

#### 18.5.2.3 Correlation coefficient

Pearson's correlation is widely used in image analysis (e.g., for comparing disparity between two images, for pattern recognition). Correlation coefficient (CR) measures linear covariation between two datasets, in this case between intensity values of the digital image of the reference object and its degraded image. Thus, higher correlation indicates that the two images have similar spatial patterns.

The *correlation coefficient* (CR) is defined as

$$CR = \frac{\sum_{i=1}^{N}(O_i - \bar{O})(I_i - \bar{I})}{\sqrt{\sum_{i=1}^{N}(O_i - \bar{O})^2}\sqrt{\sum_{i=1}^{N}(I_i - \bar{I})^2}} = \frac{\sigma_{OI}}{\sigma_O \sigma_I} \tag{18.47}$$

where $\sigma_{OI} = (1/n)\sum_{i=1}^{N}(O_i - \bar{O})(I_i - \bar{I})$ is the covariance between object $O$ and image $I$, and $\sigma_O$ and $\sigma_I$ are the standard deviation of $O$ and $I$, respectively. Thus, CR is the covariance of the two variables divided by the product of their standard deviations. The coefficient has the value of 1 if the two images are absolutely identical and 0 if they are completely uncorrelated.

### 18.5.3 OTHER SIMILARITY MEASURES

#### 18.5.3.1 Mutual information

The *mutual information* (MI) between two variables is a concept with roots in information theory and essentially measures the amount of information that one variable contains about another (Papoulis 1991). It has emerged in recent years as an effective similarity measure for comparing images.

If the intensity distributions of the object and their simulated image are taken normalized to total energy equal to 1, the MI is defined as

$$MI = H_O + H_I - H_{OI} \tag{18.48}$$

where $H_O$ and $H_I$ are the *marginal entropies* of object and image, respectively:

$$H_O = -\sum_{i=1}^{N} O_i \log O_i, \quad H_I = -\sum_{i=1}^{N} I_i \log I_i \tag{18.49}$$

and $H_{OI}$ is called the *joint entropy*:

$$H_{OI} = -\sum Hist(O,I) \cdot \log Hist(O,I) \tag{18.50}$$

or entropy of the *joint histogram*, $Hist(O,I)$, which represents the probability distribution containing the number of simultaneous occurrences of intensities between the two maps.

#### 18.5.3.2 Receiver operator methods

The *receiver operating characteristic* (ROC) is a method to evaluate the performance of a detection/imaging algorithm (Fawcett 2006). It has been a fundamental evaluation tool in clinical medicine. The ROC analysis consists of measuring the binary response of the system (target present or not) to one stimulus, for example, a reference image. First, both the reference and response images are transformed by applying a binary mask that labels pixels as background (value = 0) or foreground (value = 1). A certain threshold is fixed to decide which pixels should be considered as foreground or background. From these two binary images, the true-positive rate (TPR) and the false-positive rate (FPR) are defined as

$$TPR = \frac{TP}{F}, \quad FPR = \frac{FN}{B} \tag{18.51}$$

where

True positive ($TP$) is the number of foreground pixels, in the reference image, the system got right in the response image

False negative ($FN$) are the foreground pixels wrongly identified as background

$F$ and $B$ are the number of foreground and background pixels in the reference image, respectively

The ROC curve plots the TPR as a function of FPR for each decision threshold. Any point of this curve is a relationship between pixels correctly classified and pixels incorrectly classified. A curve located near of top left corner presents better performance compared to another one that is further away. The ROC curve is a two-dimensional depiction of imaging performance. A practical measure of the global performance by a single scalar value is given by the *area under the curve* of the ROC curve.

In particular, the ROC method can be applied to evaluate the performance of the optical system of the eye to produce

faithful images. Let $MO$ be the reference binary mask for an object (with $F$ foreground pixels and $B$ background pixels) and $MI$ the response mask for its simulated retinal image at a certain threshold setting. Then the pixel-to-pixel comparison gives

$$TPR(t) = \frac{1}{F}\sum_{i=1}^{N} MO_i \cdot MI_i, \quad FPR(t) = \frac{1}{B}\sum_{i=1}^{N} MO_i \cdot (1 - MI_i) \tag{18.52}$$

where $t$ is a decision/threshold parameter.

#### 18.5.3.3 Structural similarity index

The *structural similarity* (SSIM) index is a method for measuring the similarity between two images (Wang et al. 2004). It is designed to improve on traditional methods like PSNR and MSE, which have proven to be inconsistent with human eye perception. SSIM is based on the hypothesis that the human visual system is highly adapted for extracting structural information.

SSIM considers image degradation as perceived change in *structural information*. Structural information is the idea that the pixels have strong interdependencies especially when they are spatially close. The SSIM metric is calculated as

$$SSIM = \frac{(2\bar{O}\bar{I} + c1)(2\sigma_{OI} + c2)}{(\bar{O}^2 + \bar{I}^2 + c1)\left(\sigma_O^2 + \sigma_I^2 + c2\right)} \tag{18.53}$$

where standard deviations and covariance are the same as defined before and $c1$ and $c2$ are two constants to avoid instability.

For image quality assessment, it is useful to apply the SSIM index locally rather than globally. Usually, it is computed within a local 8 × 8 square local window, which moves pixel by pixel over the entire image.

## 18.6 VISUAL METRICS

The human system contributes to the overall image-transfer process. The problem thus becomes psychophysical in addition to physical and requires a whole approach (Millodot 2009). In this section, we introduce metrics for measuring subjectively the visual performance and some objective metrics that take into account properties of the neural visual system.

### 18.6.1 VISUAL RESOLUTION

#### 18.6.1.1 Minimum angle of resolution

The *minimum angle of resolution* (MAR) is the smallest separation between two closely high-contrast spaced details (points, lines, etc.) so that a subject is able to distinguish them as distinct. This measure does not correspond exactly with the spatial resolution defined previously because the MAR incorporates the visual factors.

When dealing with object patterns consisting of letters or gratings, the MAR is the smallest gap between letter strokes or grating bars that can be detected/resolved.

The MAR is often expressed in a logarithm scale. The *logMAR* is defined as the logarithm with base 10 of the MAR.

#### 18.6.1.2 Visual acuity

Visual acuity is the spatial resolving capacity of the visual system, that is, the ability of the eye to see fine detail. There are various ways to specify visual acuity, depending on the type of acuity task used. The most common is the *decimal visual acuity* (VA), defined as the inverse of the MAR expressed in minutes of arc:

$$VA = \frac{1}{MAR} \tag{18.54}$$

For example, if the $MAR$ = 1 minute of arc, the $VA$ = 1. A subject with $VA$ = 2 can resolve 0.5 minutes of arc between two high-contrast points.

#### 18.6.1.3 Snellen fraction

It is a measure of visual acuity based on a particular test pattern called the Snellen chart. The *Snellen fraction* (SF) is defined as

$$SF = \frac{D}{d} \tag{18.55}$$

where

$D$ is the distance at which the test is placed

$d$ is the distance at which the smallest resolved detail subtends an angle of 1 minute of arc (the smallest optotype of the Snellen chart identified subtends an angle of 5 minutes of arc)

For the small angles involved, we can replace the tangent by its argument, so the SF is practically equivalent to the decimal visual acuity:

$$SF \approx AV = \frac{1}{MAR} \tag{18.56}$$

In the most familiar acuity test, a Snellen chart is placed at a standard distance of 20 ft in the United States, or 6 m in the rest of the world. At this distance, the letters representing normal acuity subtend an angle of 5 minutes of arc, and the thickness of the strokes and of the interspaces subtends 1 minute of arc. This level is designated 20/20 (in the United States) or 6/6 (in the rest of world) and is the smallest line that a person with normal acuity can read at a distance of 20 ft.

Again, the target image is displayed at high contrast (black letters on a white background). Difficulty may occur for decreased contrast (e.g., gray letters on a white background) in spite of normal visual acuity. This is because a subsequent contrast sensitivity exam is required for describing complete visual function.

#### 18.6.1.4 Grating acuity

The *maximum resolved frequency* is the maximum spatial frequency, $f_{res}$, detected when the eye observes sinusoidal or square gratings of 100% contrast. It is related with the visual acuity and the MAR by

$$f_{res} = \frac{30}{MAR} = 30 \cdot VA \text{ cycles/degree} \tag{18.57}$$

The maximum resolved frequency by a subject is lower than the cutoff frequency, which only takes into account the optical

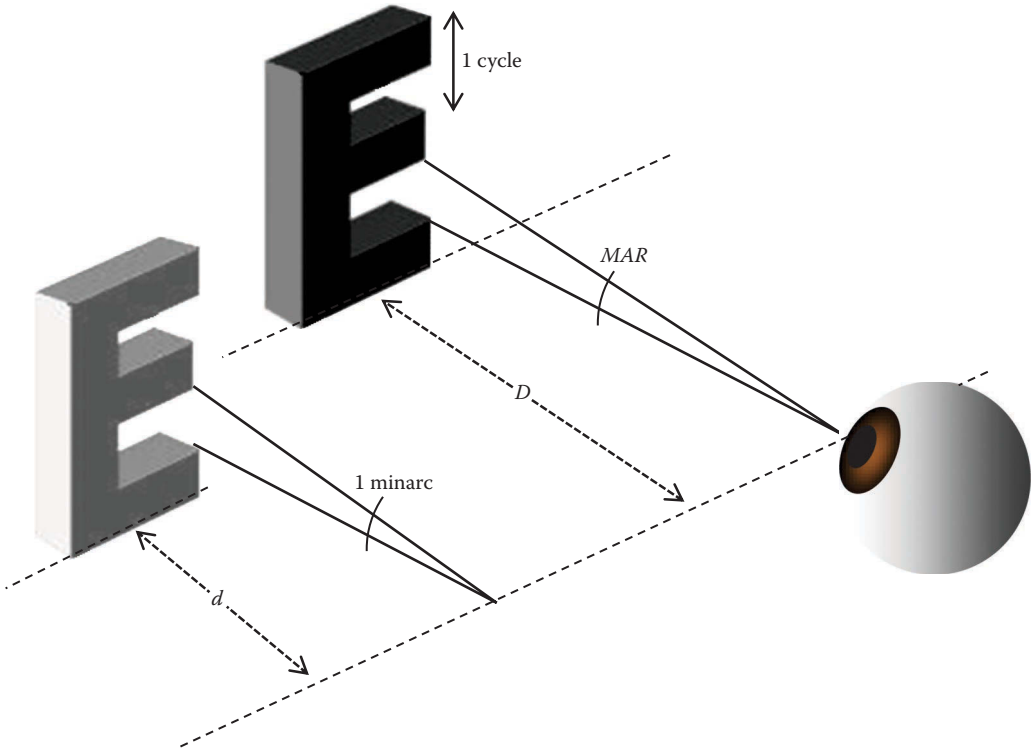


Figure 18.9 Concepts of minimum angle of resolution, visual acuity, and Snellen fraction.

factors. For instance, a subject with typical normal visual acuity of 1 can resolve a grating of 30 cycles/degree, although the MTF of its eye showed a cutoff frequency of 40 cycles/degree.

#### 18.6.1.5 Measuring visual resolution and acuity: Charts and optotypes

A variety of test patterns are used for determining the visual resolution of the human eye (Duane et al. 1998). Most of them are based on single *optotypes*, which are standardized symbols (such as letters), or charts that contain several optotypes. A condition in all of these tests is that the image is shown with 100% contrast. The most common optotypes and charts are the two-point test, the Köning optotype, the Foucault grating, the Landolt C, the Snellen E, the logMAR chart, and the Snellen chart.

For example, a 20/20 Snellen letter has a bar/stroke width of 1 minute of arc, a letter height of 5 minutes of arc, 2.5 cycles, a grating period of 2 minutes of arc (1/30 degrees), and a grating spatial frequency of 30 cycles/degree (Figure 18.9).

### 18.6.2 CONTRAST SENSITIVITY FUNCTION

#### 18.6.2.1 Threshold contrast

Suppose a visual target on a uniform background. The contrast of the target quantifies its relative difference in luminance from the background. It may be specified as *Michelson contrast*, as defined previously, $C = (I_{max} - I_{min})/(I_{max} + I_{min})$, or as *Weber contrast*. The Weber contrast is

$$C_W = \frac{I_{fore} - I_{back}}{I_{back}} \tag{18.58}$$

where $I_{fore}$ and $I_{back}$ are the intensity values for the foreground of the pattern and the background, respectively. This measure is also referred to as *Weber fraction*.

Weber contrast is claimed to be accurate for small dark symbols on a light background, where the viewer is assumed to be adapted to the background. Michelson contrast assumes the viewer is adapted to the sum of the background and foreground. Thus, Weber contrast is preferred for letter stimuli, whereas Michelson contrast is preferred for gratings.

The *threshold contrast* is the contrast required to see a target reliably. For gratings and periodic patterns, it is the minimum contrast that can be detected by the subject at a certain spatial frequency. The complete curve that plots the contrast threshold for all the spatial frequencies is the *contrast threshold function* (CTF).

#### 18.6.2.2 Contrast sensitivity function

The reciprocal of the minimum perceptible contrast is called *sensitivity* (Pelli and Bex 2013). The *contrast sensitivity function* (CSF) tells us how sensitive we are to the various frequencies of visual stimuli or, stated equivalently, tells us what is the maximum spatial frequency that we can see for each possible value of contrast. The CSF is the reciprocal of the CTF.

If the frequency of visual stimuli is too high, we will not be able to recognize the stimuli pattern any more even if it has 100% contrast. The *cutoff frequency of the CSF* ($f_{cutoff\,CSF}$) is the maximum resolved frequency and, therefore, indicates the visual acuity for maximum contrast:

$$CSF(f_{cutoff\,CSF}) = 1 \tag{18.59}$$

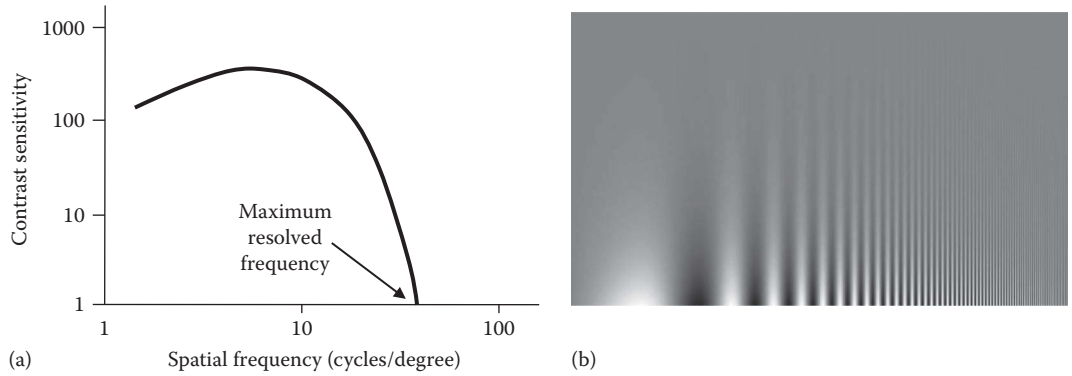


Figure 18.10 (a) From the contrast sensitivity function (CSF), different visual metrics can be defined: the maximum resolved frequency (which gives the visual acuity), the area under the CSF, the threshold contrast (reciprocal of the sensitivity) at some spatial frequency, etc. (b) The Campbell–Robson contrast sensitivity chart. Horizontal axis is spatial frequency; vertical axis is contrast.

The normal human contrast sensitivity shows a typical band-pass filter shape peaking at around 4 cycles/degree, and dropping off either side of the peak, and has a cutoff frequency between 25 and 50 cycles/degree.

For illustrating all the information carried by the CSF, we can discuss some points from the example shown in Figure 18.10. The maximum resolved frequency (sensitivity = 1) is 40 cycles/degree, which means a visual acuity of 1.33, Snellen acuity of 20/15, and minimum resolved angle of 0.75 minutes of arc. For a stimulus of 10 cycles/degree the sensitivity is 250, that is, the contrast threshold is 0.004. The example may be discussed in reverse: if the stimulus has contrast equal to 0.004, the maximum perceptible frequency is no longer 40 cycles/degree but 10 cycles/degree (i.e., we can speak of a *low-contrast VA* that would be 0.33 here).

As a rule, all contrasts and frequencies corresponding to points in the area enclosed by the CSF are visible.

Although the VA is a very important parameter, it is not sufficient to fully characterize the spatial vision. The usefulness of the CSF is that it reports the visual response for all conditions of contrast. From a clinical point of view, the CSF has great relevance because some diseases that are not detected by measuring the VA can be diagnosed and followed by means of the CSF.

#### 18.6.2.3 Neural contrast functions

The *neural contrast sensitivity function* (NCSF), or neural CSF, reflects the contrast sensitivity of the neural visual system alone, without the optical effects (Campbell and Green 1965).

The *neural transfer function* (NTF), or *neural contrast threshold function*, is the reciprocal of the neural CSF and describes the contrast threshold or contrast transfer considering the neural factors alone.

The CSF can be calculated as the product of the optical MTF and the neural CSF:

$$CSF = MTF \cdot NCSF = \frac{MTF}{NTF} \qquad (18.60)$$

#### 18.6.2.4 Measuring contrast sensitivity and affecting factors

The CSF is measured using sinusoidal gratings of variable contrast and spatial frequency (Wandell 1995). This can be done using a computer/display system or with printed charts containing stimuli of different frequencies and contrasts. In order to estimate a contrast threshold, the observer is tested over many trials, at various contrasts. Each trial is at some contrast and is scored right or wrong. The proportion of correct responses at each contrast is recorded. The observer's probability of correct response as a function of contrast is the *psychometric function*. The inverse of contrast threshold thus determined is the sensitivity. The NCSF can be measured subjectively by an interference fringe technique, which theoretically allows a sinusoidal pattern of very high contrast to be projected directly on the retina. In this way the results are not affected by aberration or diffraction from the eye's optics.

In addition to the optical factors that limit the ocular MTF and, therefore, the CSF (aberrations, pupil size, and wavelength), there are several others that affect the contrast sensitivity, such as luminance, adaptation, and visual field size. This means that determination of any visual metric must specify all these conditions.

### 18.6.3 MORE VISUAL METRICS

#### 18.6.3.1 Area between the MFT and the contrast threshold

The intersection of the MTF and the NTF gives the highest spatial frequency for which the MTF is above the neural threshold. We call this the *crossover frequency* ($f_{cross}$) and is exactly the cutoff frequency of the CSF ($f_{cutoffCSF}$) defined before.

The area between the MFT and the neural contrast threshold function (or NTF) between zero and the crossover frequency is mathematically defined as

$$Area(MTF - NTF) = \int_0^{fcross} [MTF(f) - NTF(f)]df \qquad (18.61)$$

The rationale behind this metric is that it summarizes the extent of signal MTF in excess of the threshold requirement of the visual system over all usable frequencies.

When computing this metric, phase-reversed segments of the MTF curve count as positive area, which makes that spurious resolution be counted as beneficial when predicting visual performance for the task of contrast detection. This metric assumes that the area is homogeneous in image quality, that is,

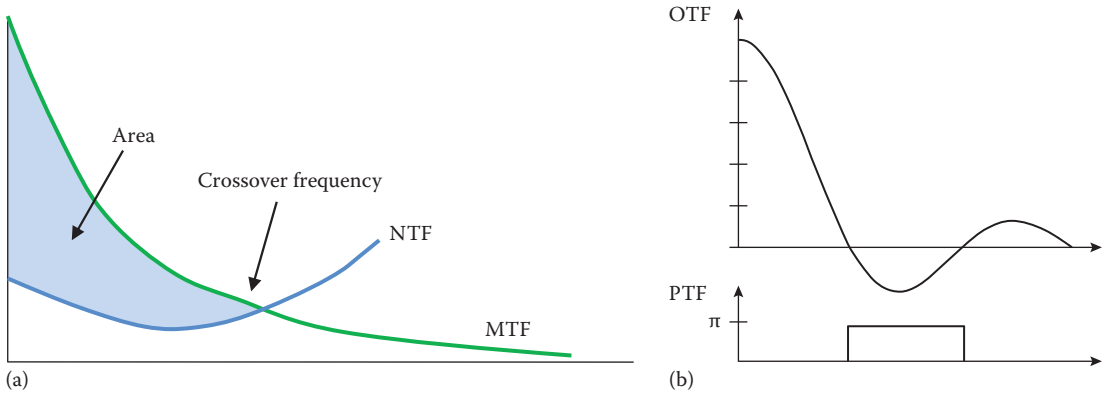


Figure 18.11 (a) Area between the modulation transfer function (MTF) and the neural contrast threshold. The rationale behind this metric is that it computes only the signal of the MTF over the usable frequencies. The crossover frequency is mathematically the cutoff frequency of the contrast sensitivity function. (b) Some visual metrics are based on the optical transfer function and are intended to discard phase-reversed contrasts.

that the excess of MTF over NTF is uniformly important for all spatial frequencies above the threshold requirement. Some authors suggested that the MTF be weighted by the spatial frequency power spectrum of the image to be seen to determine an effective area. On the other hand, it has been shown that it is important to have adequate signal above that minimally required for detection, but additional increases in this excess of MTF over NTF are of less value in many real-world tasks. This idea leads to define similar metrics by computing the MTF area only in a region near the threshold (Figure 18.11).

### 18.6.3.2 Subjective quality factor

Granger proposed a single metric that would correlate with perceived image quality (Granger and Cupery 1972). In his definition, *subjective quality factor* (SQF) defines a pass-band filter that is constructed by averaging the MTF between the peak frequency of the CSF and four times that frequency. More exactly, the SQF is the area of the MTF from $f1 = 0.5$ cycles/mm (1.7 cycle/degree) to $f2 = 2$ cycles/mm (6.7 cycles/degree):

$$SQF = \int_{f1}^{f2} MTF(f)d(\log f) \qquad (18.62)$$

This factor and the area between the MFT and the NTF are concepts originally developed for photographic systems, generalized to electro-optical system applications and image quality tasks.

### 18.6.3.3 Other metrics based on area

The *area between the OTF and the contrast threshold* is (Thibos et al. 2004)

$$Area(OTF - NTF) = \int_{0}^{fcross} [OTF(f) - NTF(f)]df \qquad (18.63)$$

where $OTF(f)$ is the radially averaged OTF, which is real valued because imaginary component vanishes after integration. The difference with the previous metric is that phase-reversed segments of the curve do not contribute to the area. Thus, this metric would be appropriate for tasks in which phase-reversed contrasts (spurious resolution) actively interfere with performance.

The *area under the CSF* is calculated as

$$Area(CSF) = \int_{0}^{fcutoff} CSF(f)df = \int_{0}^{fcutoff} MTF(f) \cdot NCSF(f)df \qquad (18.64)$$

This is the same than the area under the MTF weighted by the neural CSF.

A metric that is intended to quantify the visually significant shifts in the image is the *area under the neurally weighted OTF* divided by the area under the neurally weighted MTF:

$$\frac{Area(OTF)_{NCSF}}{Area(CSF)} = \frac{\int_{0}^{fcutoff} OTF(f) \cdot NCSF(f)df}{\int_{0}^{fcutoff} MTF(f) \cdot NCSF(f)df} = \frac{\int_{0}^{fcutoff} OTF(f) \cdot NCSF(f)df}{Area(CSF)} \qquad (18.65)$$

The *visual Strehl ratio* (VSR) is similar to the OTF method of computing the SR, except that the OTF is weighted by the NCSF:

$$VSR = \frac{\int_{-\infty}^{\infty}\int_{-\infty}^{\infty} OTF(u,v) \cdot NCSF(u,v)du\,dv}{\int_{-\infty}^{\infty}\int_{-\infty}^{\infty} OTF_{d-l}(u,v) \cdot NCSF(u,v)du\,dv} \qquad (18.66)$$

### 18.6.3.4 Neural sharpness

*Neural sharpness* (NS) was introduced as a way to capture the effectiveness of a PSF for stimulating the neural portion of the visual system (Williams et al. 2003). It is the maximum value of

the convolution of the eye's PSF and a spatial sensitivity function with a Gaussian profile that represents the neural visual system:

$$NS = \max(PSF * g) \tag{18.67}$$

where $g(x,y)$ is a bivariate Gaussian weighting function with a standard deviation of 1 minute of arc, which effectively ignores light outside of the central 4 minutes of arc of the PSF.

### 18.6.4 POLYCHROMATIC METRICS

The WA for each wavelength is treated separately because lights of different wavelengths are mutually incoherent. For this reason, metrics of wavefront quality do not generalize easily to the case of polychromatic light. However, there have been several attempts to characterize the image quality of the human eye including the longitudinal and the transverse chromatic aberrations (Font et al. 1994; Marcos et al. 1999; Ravikumar et al. 2008; Van Meeteren 1974).

The *polychromatic point spread function* may be computed as the superposition of the monochromatic PSFs for each wavelength defocused by axial chromatic aberration and shifted by lateral chromatic aberration:

$$PSF_{poly}(x, y) = \sum_{\lambda} PSF_{\lambda}(x, y) \tag{18.68}$$

A different approach is to incorporate the effect of the human spectral sensitivity and calculate the polychromatic PSF as the weighted sum:

$$PSF_{poly} = \int_{\lambda 1}^{\lambda 2} PSF(\lambda) \cdot V(\lambda) d\lambda \tag{18.69}$$

where $V(\lambda)$ is the luminous efficiency as function of wavelength (Thibos et al. 2004).

These definitions may be substituted in any of the equations given above to produce new polychromatic metrics of image quality. For example, the *polychromatic MTF* may be computed as the modulus of the FT of the polychromatic PSF. Also, simulated images in white light are easily derived from their monochromatic counterparts.

## 18.7 SUMMARY AND EXAMPLES OF APPLICATIONS

A problem of considering the aberration coefficients or the statistical parameters of the WA is that one does not know a priori what will be the appearance of the image formed by the system. As we have already noted, there is not a trivial relationship between optical quality and image quality. For example, balancing aberrations does not always lead to improved images. Also it occurs that some aberration terms may degrade the image more than others even if both have the same magnitude. However, optical metrics have proven to be useful in many applications in vision. For example, the analysis at the optical level of the astigmatism change or the coma induced by an incision of cataract surgery, or by refractive surgery, allows gaining insight for improving these treatments that act on the optical surfaces of the eye. Some of the numerous works that have studied optical quality of the human eye in terms of the aberration coefficients or the RMS of the WA are, for instance, the relative contribution of the spherical aberration of cornea and lens (Artal et al. 2001), optical aberrations of the human cornea as a function of age (Guirao et al. 2000), spherical aberration versus accommodation (Cheng et al. 2004a; He et al. 2000), the limits to a perfect ideal customized wavefront correction due to the change of aberrations during accommodation (Artal et al. 2002), optical quality of intraocular lenses for pseudophakic eyes in terms of its spherical aberration (Piers et al. 2004), comparative study of changes in coma after cataract surgery (Guirao et al. 2004), the distribution of the eye's aberrations in the normal population (Porter et al. 2001), and a "virtual surgery" approach designed to predict optical performance in pseudophakic eyes (Tabernero et al. 2006).

Metrics defined on the image plane or in the frequency domain are intended to quantify optical performance regardless of optical quality. Some applications to vision of metrics that are based on the PSF are retinal image quality in patients implanted with intraocular lenses in terms of the PSF and the SR (Guirao et al. 2002a), off-axis aberrations estimated from double-pass measurements of the PSF (Guirao and Artal 1999), the HWHM of the double-pass PSF in subjects after correction of the ocular aberrations with adaptive optics (Logean et al. 2008), depth from focus based on entropy (Bove 1993), EE to investigate the optimal amount of spherical aberration for design of intraocular lenses (Wang and Koch 2007), etc. Also, entropy, SR, and intensity variance of the PSF have been used for predicting subjective image quality (Chen et al. 2005) and refractive errors from WA data (Guirao and Williams 2003).

Examples of metrics based on grating objects and the MTF can be found in the following works: the area under the MTF between 0 and 60 cycles/degree has been applied to predict subjective image quality (Chen et al. 2005) and refractive errors (Guirao and Williams 2003), a method has been proposed to determine intraocular lens power by maximizing the area under the MTF (Canovas and Artal 2011), the visual benefit of correcting higher-order aberrations of the eye was evaluated from the MTF at 16 and 32 cycles/degree (Guirao et al. 2002b) and from the HR at 16 cycles/degree (Williams et al. 2000), also the MTF at 16 cycles/degree was used to evaluate the "effective correction" of a laser beam in laser refractive surgery (Guirao et al. 2003), the pseudo SR computed from MTF areas ($SR_{MTF}$) was applied for quantifying optical performance of the aging eye (Guirao et al. 1999), and metrics based on the volume under the MTF have been used in studies of chromatic aberration (Marcos et al. 1999) and visual instrumentation (Mouroulis 1999).

The simulation of retinal images by computational convolution is a common method for estimating image quality. For example, the convolved images of the letter "E" based on the measured aberrations have been used to simulate vision in keratoconic eyes (Sabesan and Yoon 2009), in LASIK patients and vision through adaptive optics (Williams et al. 2000), or the peripheral image quality (Jaeken et al. 2013).

Objective image quality metrics for evaluating processed images are preferred to subjective evaluation, which is slow and

inconvenient for practical usage. The most common computable objective measures of image quality are the mean square error and the PSNR. These distance metrics are often used for quality evaluation of medical images and retinal images (Nirmala et al. 2014). However, their predictions often do not agree well with the human visual perception. Image quality assessment can be improved by incorporating some models of human visual system. The SSIM index has been proposed, for example, to evaluate the subjective perception of quality of natural images (Wang et al. 2004). The MI was applied to registration of retinal images (Zhu 2007).

Faithful determination of visual performance depends on subjective or psychophysical measurements because of the visual system processing. Visual metrics such as the area under the CSF, or the polychromatic PSF and MTF, have been used, for example, to evaluate the effect of rotation and translation on the expected benefit of correcting the ocular aberrations (Guirao et al. 2001). The VSR accounted for visual acuity (Marsack et al. 2004) and predicted subjective refraction (Thibos et al. 2004). It has been measured the ability of the NS and the VSR to predict high- and low-contrast acuity (Applegate et al. 2006) and the impact of aberrations on subjective image quality by means of the NS (Chen et al. 2005).

The relationship between objective and subjective visual performance is being increasingly investigated. Just for mentioning a few works: the application of optical quality metrics to predict subjective quality of vision after laser in situ keratomileusis (Bühren et al. 2009), the SR of the PSF generated at rotated versions of aberrations support the hypothesis that the neural visual system is adapted to the eye's aberrations (Artal et al. 2004), the effect on visual performance of the interactions between aberrations (Applegate et al. 2003), the impact of higher-order aberrations on subjective best focus (Cheng et al. 2004b), estimation of visual quality from wavefront aberrations (Cheng et al. 2003), the impact of positive coupling of the eye's trefoil and coma in retinal image quality and visual acuity (Villegas et al. 2012), the effect of chromatic aberration on visual acuity (Campbell and Gubisch 1967) and visual performance (Thibos et al. 1991), etc.

## REFERENCES


Applegate, R. A., Marsack, J. D., and Thibos, L. N., Metrics of retinal image quality predict visual performance in eyes with 20/17 or better visual acuity, *Opt. Vis. Sci.* 83 (2006): 635–640.

Applegate, R. A., Marsack, J. D., Ramos, R., and Sarver, E. J., Interactions between aberrations can improve or reduce visual performance, *J. Cataract Refract. Surg.* 29 (2003): 1487–1495.

Artal, P., Optics of the eye and its impact in vision: A tutorial, *Adv. Opt. Photon.* 6 (2014): 340–367.

Artal, P., Understanding aberrations by using double-pass techniques, *J. Refract. Surg.* 16 (2000): S560–S562.

Artal, P., Chen, L., Fernández, E. J. et al., Neural compensation for the eye's optical aberrations, *J. Vis.* 4 (2004): 281–287.

Artal, P., Fernández, E. J., and Manzanera, S., Are optical aberrations during accommodation a significant problem for refractive surgery? *J. Refract. Surg.* 18 (2002): S563–S566.

Artal, P., Guirao, A., Berrio, E., and Williams, D. R., Compensation of corneal aberrations by the internal optics in the human eye, *J. Vis.* 1 (2001): 1–8.

Barakat, R., Some entropic aspects of optical diffraction imagery, *Opt. Commun.* 156 (1998): 235–239.

Bareket, N., Second moment of the diffraction point spread function as an image quality criterion, *J. Opt. Soc. Am.* 69 (1979): 1311–1312.

Born, M. and Wolf, E., *Principles of Optics*. Cambridge, U.K.: Cambridge University Press, 1999.

Bove, V. M., Entropy-based depth from focus, *J. Opt. Soc. Am. A* 10 (1993): 561–566.

Bühren, J., Pesudovs, K., Martin, T., Strenger, A., Yoon, G., and Kohnen, T., Comparison of optical quality metrics to predict subjective quality of vision after laser in situ keratomileusis, *J. Cataract Refract. Surg.* 35 (2009): 846–855.

Campbell, F. W. and Green, D. G., Optical and retinal factors affecting visual resolution, *J. Physiol.* 181 (1965): 576–593.

Campbell, F. W. and Gubisch, R. W., The effect of chromatic aberration on visual acuity, *J. Physiol.* 192 (1967): 345–358.

Canovas, C. and Artal, P., Customized eye models for determining optimized intraocular lenses power, *Biomed. Opt. Express* 2 (2011): 1649–1662.

Charman, W. N. and Jennings, J. A. M., The optical quality of the monochromatic retinal image as a function of focus, *Br. J. Physiol. Opt.* 31 (1976): 119–134.

Chen, L., Singer, B., Guirao, A., Porter, J., and Williams, D. R., Image metrics for predicting subjective image quality, *Optom. Vis. Sci.* 82 (2005): 358–369.

Cheng, H., Barnett, J. K., Vilupuru, A. S. et al., A population study on changes in wave aberrations with accommodation, *J. Vis.* 4 (2004a): 272–280.

Cheng, X., Bradley, A., and Thibos, L. N., Impact of higher order aberration on subjective best focus, *J. Vis.* 4 (2004b): 310–321.

Cheng, X., Thibos, L. N., and Bradley, A., Estimating visual quality from wavefront aberration measurements, *J. Refract. Surg.* 19 (2003): 579–584.

CIE (Commission Internationale de l'Éclairage). *ILV: International Lighting Vocabulary*. Vienna, Austria: CIE S 017/E, 2011.

Corbin, J. A., Klein, S., and van de Pol, C., Measuring effects of refractive surgery on corneas using Taylor series polynomials, *Proc. SPIE*, 3591 (1999): 46–52.

Driggers, R. G., *Encyclopedia of Optical Engineering*. New York: Marcel Dekker, 2003.

Duane, T. D., Tasman, W., and Jaeger, E. A., *Duane's Foundations of Clinical Ophthalmology*. Philadelphia, PA: Lippincott, Williams & Wilkins, 1998.

Fawcett, T., An introduction to ROC analysis, *Pattern Recognit. Lett.* 27 (2006): 861–874.

Fienup, J. R. and Miller, J. J., Aberration correction by maximizing generalized sharpness metrics, *J. Opt. Soc. Am. A* 20 (2003): 609–620.

Font, C., Escalera, J. C., and Yzuel, M. J., Polychromatic point spread function: Calculation accuracy, *J. Modern Opt.* 41 (1994): 1401–1413.

Gonzalez, R. C., *Digital Image Processing*. Upper Saddle River, NJ: Pearson Prentice Hall, 2008.

Goodman, J. W., *Introduction to Fourier Optics*. New York: McGraw-Hill, 1996.

Granger, E. M. and Cupery, K. N., An optical merit function (SQF) which correlates with subjective image judgements, *Photogr. Sci. Eng.* 16 (1972): 221–230.

Guirao, A. and Artal, P., Off-axis monochromatic aberrations estimated from double pass measurements in the human eye, *Vis. Res.* 39 (1999): 207–217.

Guirao, A., González, C., Redondo, M., Geraghty, E., Norrby, S., and Artal, P., Average optical performance of the human eye as a function of age in a normal population, *Invest. Ophthalmol. Vis. Sci.* 40 (1999): 203–213.

Guirao, A., Porter, J., Williams, D. R., and Cox, I. G., Calculated impact of higher-order monochromatic aberrations on retinal image quality in a population of human eyes, *J. Opt. Soc. Am. A* 19 (2002b): 1–9.

Guirao, A., Redondo, M., and Artal, P., Optical aberrations of the human cornea as a function of age, *J. Opt. Soc. Am. A* 17 (2000): 1697–1702.

Guirao, A., Redondo, M., Geraghty, E., Piers, P., Norrby, S., and Artal, P., Corneal optical aberrations and retinal image quality in patients in whom monofocal intraocular lenses were implanted, *Arch. Ophthalmol.* 120 (2002a): 1143–1151.

Guirao, A., Tejedor, J., Artal, P., Corneal aberrations before and after small-incision cataract surgery, *Invest. Ophthalmol. Vis. Sci.* 45 (2004): 4312–4319.

Guirao, A. and Williams, D. R., A method to predict refractive errors from wave aberration data, *Optom. Vis. Sci.* 80 (2003): 36–42.

Guirao, A., Williams, D. R., and Cox, I. G., Effect of rotation and translation on the expected benefit of an ideal method to correct the eye's higher-order aberrations, *J. Opt. Soc. Am. A* 18 (2001): 1003–1015.

Guirao, A., Williams, D. R., and MacRae, S. M., Effect of beam size on the expected benefit of customized laser refractive surgery, *J. Refract. Surg.* 19 (2003): 15–23.

He, J. C., Burns, S. A., and Marcos, S., Monochromatic aberrations in the accommodated human eye, *Vis. Res.* 40 (2000): 41–48.

Helmholtz, H. V., *Popular Lectures on Scientific Subjects*. New York: Appleton, 1885.

Hopkins, H. H., The use of diffraction-based criteria of image quality in automatic optical design, *Opt. Acta* 13 (1966): 343–369.

Howland, H. C. and Howland, B., A subjective method for the measurement of monochromatic aberrations of the eye, *J. Opt. Soc. Am. A* 67 (1977): 1508–1518.

Iglesias, I., Lopez-Gil, N., and Artal, P., Reconstruction of the ocular PSF from a pair of double pass retinal images, *J. Opt. Soc. Am. A* 15 (1998): 326–339.

Jaeken, B., Mirabet, S., Marín, J. M., and Artal, P., Comparison of the optical image quality in the periphery of Phakic and Pseudophakic eyes, *Invest. Ophthalmol. Vis. Sci.* (2013) 54: 3594–3599.

Lisson, J. B., and Mounts, D. I., Estimation of imaging performance using local optical quality factor metrics, *Opt. Eng.* 31 (1992): 1038–1044.

Logean, E., Dalimier, E., and Dainty, C., Measured double-pass intensity point-spread function after adaptive optics correction of ocular aberrations, *Opt. Express* 16 (2008): 17348–17357.

Mahajan, V. N., *Aberration Theory Made Simple*. Bellingham, WA: SPIE Press, 1991.

Mahajan, V. N., *Optical Imaging and Aberrations*. Bellingham, WA: SPIE Press, 1998.

Mahajan, V. N., Strehl ratio for primary aberrations: Some analytical results for circular and annular pupils, *J. Opt. Soc. Am.* 72 (1982): 1258–1266.

Malacara, D., *Optical Shop Testing*. New York: John Wiley & Sons Inc., 1992.

Marcos, S., Burns, S. A., Moreno-Barriuso, E., and Navarro, R., A new approach to the study of ocular chromatic aberrations, *Vis. Res.* 39 (1999): 4309–4323.

Marsack, J. D., Thibos, L. N., and Applegate, R. A., Metrics of optical quality derived from wave aberrations predict visual performance, *J. Vis.* 4 (2004): 322–328.

Millodot, M., *Dictionary of Optometry and Visual Science*. Oxford, U.K.: Butterworth-Heinemann, 2009.

Mouroulis, P., *Visual Instrumentation: Optical Design & Engineering Principles*. New York: McGraw-Hill, 1999.

Nirmala, S. R., Dandapat, S., and Bora, P. K., Quality measures for retinal images, in *Ophthalmological Imaging and Applications*, E. Y. K. Ng et al., eds., Chapter 4. Boca Raton, FL: CRC Press, 2014.

Papoulis, A., *Probability, Random Variables, and Stochastic Processes*. New York: McGraw-Hill, 1991.

Pelli, D. G. and Bex, P., Measuring contrast sensitivity, *Vis. Res.* 90 (2013): 10–14.

Piers, P. A., Fernández, E. J., Manzanera, S., Norrby, S., and Artal, P., Adaptive optics simulation of intraocular lenses with modified spherical aberration, *Invest. Ophthalmol. Vis. Sci.* 45 (2004): 4601–4610.

Porter, J., Guirao, A., Cox, I. G., and Williams, D. R., Monochromatic aberrations of the human eye in a large population, *J. Opt. Soc. Am. A* 18 (2001): 1793–1803.

Ravikumar, S., Thibos, L. N., and Bradley, A., Calculation of retinal image quality for polychromatic light, *J. Opt. Soc. Am. A* 25 (2008): 2395–2407.

Sabesan, R. and Yoon, G., Visual performance after correcting higher order aberrations in keratoconic eyes, *J. Vis.* 9 (2009): 1–10.

Shannon, R. R., *The Art and Science of Optical Design*. Cambridge, U.K.: Cambridge University Press, 1997.

Siegman, A. E., How to (maybe) measure laser beam quality, in *DPSS (Diode Pumped Solid State) Lasers: Applications and Issues*, M. Dowley, ed., Vol. 17 of OSA Trends in Optics and Photonics, Washington D.C.: Optical Society of America 1998, paper MQ1.

Smith, W. J., *Modern Optical Engineering*. New York: McGraw-Hill Professional, 2000.

Srisailam, A., Dharmaiah, V., Ramanamurthy, M. V., and Mondal, P. K., Encircled energy factor as a point-image quality-assessment parameter, *Adv. Appl. Sci. Res.* 2 (2011): 145–154.

Tabernero, J., Piers, P., Benito, A., Redondo, M., and Artal, P., Predicting the optical performance of eyes implanted with IOLs to correct spherical aberration, *Invest. Ophthal. Visual Sci.* 47 (2006): 4651–4658.

Thibos, L. N., Bradley, A., and Zhang, X., Effect of ocular chromatic aberration on monocular visual performance, *Optom. Vis. Sci.* 68 (1991): 599–607.

Thibos, L. N., Hong, X., Bradley, A., and Applegate, R. A., Accuracy and precision of objective refraction from wavefront aberrations, *J. Vis.* 4 (2004): 329–351.

Van Meeteren, A., Calculations of the optical modulation transfer function of the human eye for white light, *Opt. Acta* 21 (1974): 395–412.

Villegas, E. A., Alcón, E., and Artal, P., Impact of positive coupling of the eye's trefoil and coma in retinal image quality and visual acuity, *J. Opt. Soc. Am. A* 29 (2012): 1667–1672.

Wandell, B. A., *Foundations of Vision*. Sunderland, MA: Sinauer Associates, 1995.

Wang, J. Y. and Silva, D. E., Wave-front interpretation with Zernike polynomials, *Appl. Opt.* 19 (1980): 1510–1519.

Wang, L. and Koch, D. D., Custom optimization of intraocular lens asphericity, *J. Cataract Refract. Surg.* 33 (2007): 1713–1720.

Wang, Z., Bovik, A. C., Sheikh, H. R., and Simoncelli, E. P., Image quality assessment: From error visibility to structural similarity, *IEEE Trans. Image Process.* 13 (2004): 600–612.

Westheimer, G. and Campbell, F. W., Light distribution in the image formed by the living human eye, *J. Opt. Soc. Am.* 52 (1962): 1040–1045.

Williams, C. S. and Becklund, O. A., *Introduction to the Optical Transfer Function*. Bellingham, WA: SPIE Press, 2002.

Williams, D. R., Applegate, R. A., and Thibos, L. N., Metrics to predict the subjective impact of the eye's wave aberration, in *Wavefront Customized Visual Correction: The Quest for Supervision II*, R.R. Krueger. R.A. Applegate, and S.M. MacRae, eds. Thorofare, NJ: Slack Inc., 2003, pp. 77–84.

Williams, D. R., Yoon, G. Y., Porter, J., Guirao, A., Hofer, H., and Cox, I. G., Visual benefit of correcting higher order aberrations of the eye, *J. Refract. Surg.* 16 (2000): 554–559.

Williams, T., *The Optical Transfer Function of Imaging Systems*. Bristol, U.K.: CRC Press, 1998.

Wyant, J. C. and Creath, K., Basic wavefront aberration theory for optical metrology, in *Applied Optics and Optical Engineering (Vol. XI)*, R.R. Shannon and J.C. Wyant, eds. Boston, MA: Academic Press, 1992, pp. 2–53.

Zhang, L., Zhang, L., Mou, X., and Zhang, D., A comprehensive evaluation of full reference image quality assessment algorithms, in *Proceedings of IEEE International Conference on Image Processing*, Orlando, FL, 2012, pp. 1477–1480.

Zhu, Y. M., Mutual information-based registration of temporal and stereo retinal images using constrained optimization, *Comput. Methods Prog. Biomed.* 86 (2007): 210–215.